Fluid Mechanics
2020; 6(2): 30-50
http://www.sciencepublishinggroup.com/j/fm
doi: 10.11648/j.fm.20200602.11
ISSN: 2575-1808 (Print); ISSN: 2575-1816 (Online)

Quinn's Law of Fluid Dynamics: Supplement #3 A Unique Solution to the Navier-Stokes Equation for Fluid Flow in Closed Conduits

Hubert Michael Quinn

Department of Research and Development, the Wrangler Group LLC, Brighton, USA

Email address:
hubert@wranglergroup.com

To cite this article:
Hubert Michael Quinn. Quinn's Law of Fluid Dynamics: Supplement #3 A Unique Solution to the Navier-Stokes Equation for Fluid Flow in Closed Conduits. *Fluid Mechanics*. Vol. 6, No. 2, 2020, pp. 30-50. doi: 10.11648/j.fm.20200602.11

Received: July 22, 2020; **Accepted**: August 5, 2020; **Published**: August 25, 2020

Abstract: The recent publication of Quinn's Law of Fluid Dynamics brings into focus longstanding contradictions regarding permeability in closed conduits that have littered the fluid dynamics landscape for more than 150 years. In this paper, we will use this new level of understanding to explain these contradictions, in layman's terms, and resolve them, by introducing for the first time, as far as we know, a unique solution to the Navier-Stokes equation for fluid flow in closed conduits, which is understandable by knowledgeable physicists, engineers, chromatographers and aerospace enthusiasts alike, but who may not necessarily be versed in the abstract jargon of a graduate in advanced mathematics. In addition, we will apply our unique solution to chosen illustrative worked examples, as well as those of third parties from the published literature. In so doing, we will demonstrate the utility of our solution, not only, to packed conduits containing particles having solid skeletons, but also, to empty conduits, which in the context of this new understanding of fluid dynamics in closed conduits, represents a special case of a packed conduit in which the particles are fully porous, i.e., they are made entirely of free space.

Keywords: Forchheimer Coefficients, Conduit Permeability, Continuity Equation, Porosity, Tortuosity, Packed Conduits

1. Introduction

Let us begin at the beginning. Most practitioners will say that the first real attempt to characterize the flow of fluids through closed conduits was made by Poiseuille circa 1846 [1], in the case of empty conduits, and by Henry Darcy in 1856 [2], in the case of conduits packed with solid obstacles. The former's work led to what is known today as Poiseuille's Law [3] and the latter's work to what is known as Darcy's Law [4]. Both these Laws teach that there is a linear relationship between fluid flow rate and the pressure drop across a given conduit. As time progressed, however, it became obvious that both these Laws had limitations, and in the intervening 170 years approximately, much effort has been devoted to ascertaining the underlying reasons [5-12]. Unfortunately, among practitioners, even to this day, there is much controversy regarding the parameters which constitute the pressure/flow relationship [13].

Darcy's original methodology used screened river sand packed into large pipes, through which he pumped water, and recorded the pressure drop across the packed pipe for each measurement of flow rate of the water [14]. It would be logical to conclude, therefore, that the precise nature of the sand particles, and the manner in which they were forced together inside the packed conduit, should be fertile ground for experimentation in any efforts to better understand the pressure/flow relationship in packed conduits [15]. Throughout the middle to end of the 20th century, Blake, Kozeny, Carman, Bird Stewart and Lightfoot, Giddings, Halasz and Guiochon are just some of the more prominent scientists who devoted considerable effort to the elucidation of a fluid flow model capable of describing accurately the elements underlying this *linear* pressure/flow relationship, i.e., that portion of the fluid flow regime where *viscous* contributions to pressure drop dominate over *kinetic* contributions [16-22]. Unfortunately, however, their efforts did not culminate in a consensus of opinion and we are left today with the glaring contradictions regarding the value of the constant in the Kozeny/Carman equation, which is generally accepted as the most popular equation to describe

the pressure/flow relationship in packed conduits, when the dominant contributions are derived from viscous sources [23, 24]. Giddings circa 1965, for instance, teaches that this value is 270 [25], while Halasz and his disciples claim that its value is 180 [26, 27], which is the value derived originally by Carman in 1937 [28]. Furthermore, the concept of conduit external porosity has been misapplied mostly in the engineering disciplines [29]. To make matters even worse, with the advent of the use of porous particles in applications like chromatographic separations, where solute molecules are separated based upon their ability to penetrate the pore network internal to the particles in a packed conduit, yet other elements of confusion have found their way into the controversy. Particle porosity, which is a variable that is independent of the packed conduit, has been invariably conflated with conduit internal porosity and "mobile phase velocity", which is not a fluid velocity of any kind, has been conflated with the fluid velocity in many chromatographic journal publications [30, 31]. In the realm of the flow regime where kinetic contributions begin to manifest, Sabri Ergun circa 1950, in combination with others, most notably Orning, produced an equation which uses the sum of two distinct terms to capture both viscous and kinetic contributions [32]. This was a significant step forward in understanding how the pressure/flow relationship changes as the fluid accelerates into the region where kinetic contribution trump viscous contributions. Sadly, however, in 1952 this development morphed into, one step forward and two steps backwards, when Ergun assigned values of 150 and 1.75 for the constants in the viscous and kinetic terms in his now famous "Ergun equation" [33]. Throughout the intervening years, these values have been shown to be un-certifiable and, consequently, have added fuel to the fire of the ever expanding controversy which litters this field of study to this very day [34].

While experimentation on packed conduits were in progress in the middle of the 20th century by the investigators mentioned above, other investigators, in parallel, were focused on the exact same objective with respect to the flow in empty conduits [35]. The efforts of Sir Osborn Reynolds, in particular, stand out, reaching back to 1883 [36]. Johan Nikuradze, for instance, is another most respected name when it comes to the fundamental experiments underlying the impact of inner wall roughness on the fluid flow profile in empty conduits. Actually, he carried out two seminal sets of experiments, circa 1933, one deals with smooth walled conduits and one deals with inner wall roughened conduits [37, 38]. Furthermore, since he was a student of Prandtl, their contributions are linked within a theory put forward by the latter, which forms the basis of their concept of the fluid boundary layer, a fluidic phenomenon that forms adjacent to a solid boundary due to viscosity, and which theory has been recognized as the father of wing flight fluid dynamics [39]. Fluid flow in empty conduits is extremely important in many engineering applications, so it is perhaps understandable that an engineer, Lewis Moody, circa 1944, building on the work of Nikuradze and others, produced the now famous "Moody diagram" which has been used as a popular "look up" chart by the engineering discipline for fluid flow designs which require knowledge of fluid flow in the region where kinetic contributions dominate [40]. The diagram is based upon the concept of "friction factor" which is a man-made entity however, being as it is a mathematical construct and, thus, unfortunately, suffers from the defects of its qualities [41]. It has, in addition, been updated from time to time since its original creation [42]. In more modern times, the Princeton Super Pipe has gained in popularity with respect to the theory of fluid dynamics in smooth pipes and has been credited with an update to the conventional concept of the "Law of the Wall" [43].

It is apparent from the brief history of the development of fluid flow theory outlined above, that empty and packed conduits formed separate and distinct categories of investigative effort involving fluid flow theory throughout the past 150 plus years. While some attempts were made to produce a unified fluid flow model which would seamlessly embrace both types of fluid flow embodiments throughout that period, none were successful, at least up until now [44]. With the advent of the Quinn Fluid Flow Model (QFFM) published last year (2019), this is no longer the case [45]. Accordingly, this paper is dedicated to elucidating a unified methodology for both packed and empty conduits, which a typical practitioner can take advantage of, whether that practitioner is an engineer, chromatographer or aerospace enthusiast.

We begin by introducing a methodology used in engineering circles called Hydraulic Conductivity [46]. To put this term in context for all disciplines, we show the relationship between hydraulic conductivity ($\Delta H/L$) and pressure gradient ($\Delta P/L$):

$$\frac{\Delta H}{L} = \frac{\Delta P}{\rho_f g L} \tag{1}$$

We can see from the right hand side of equation (1) that hydraulic conductivity involves, not only, the pressure gradient across a packed conduit, but also, includes the fluid density, and the acceleration due to gravity. Thus, from an empirical perspective, a practitioner need only measure the pressure drop at any given flow rate, the length of the conduit, and obtain from reference text books the value for the density of the fluid used in the measurement, as well as the acceleration due to gravity. In addition, since it is customary when carrying out permeability determinations in packed conduits, to record the measured flow rate corresponding to the measured pressure drop, as fluid flux through the packed conduit, plotting fluid flux versus hydraulic conductivity is a popular engineering methodology. Thus, we can write:

$$\mu_s = \frac{4q}{\pi D^2} \tag{2}$$

Where equation (2) represents the fluid flux, also called linear superficial fluid velocity, q=volumetric fluid flow rate, D=the conduit diameter.

Accordingly, in order to use the fluid flux parameter, the

practitioner must measure, in addition to the fluid volumetric flow rate, the conduit diameter.

2. Methods

When reporting empirical results of permeability in packed conduits, the Forchheimer fluid flow model is a popular engineering methodology, especially when the fluid flow regime involves significant kinetic contributions [47]. We can write the Forchheimer equation as follows:

$$\frac{\Delta H}{L} = a\mu_s + b\mu_s^2 \quad (3)$$

Normalizing equation (3) by dividing across by μ_s, gives:

$$\frac{\Delta H}{L\mu_s} = a + b\mu_s \quad (4)$$

Where, a, and b, are the Forchheimer coefficients for the viscous and kinetic contributions, respectively.

Thus, we can see from equation (3) that hydraulic conductivity is a quadratic function of fluid flux. It is customary in engineering circles to make a plot of equation (3), a typical example of which is shown in Figure 1.

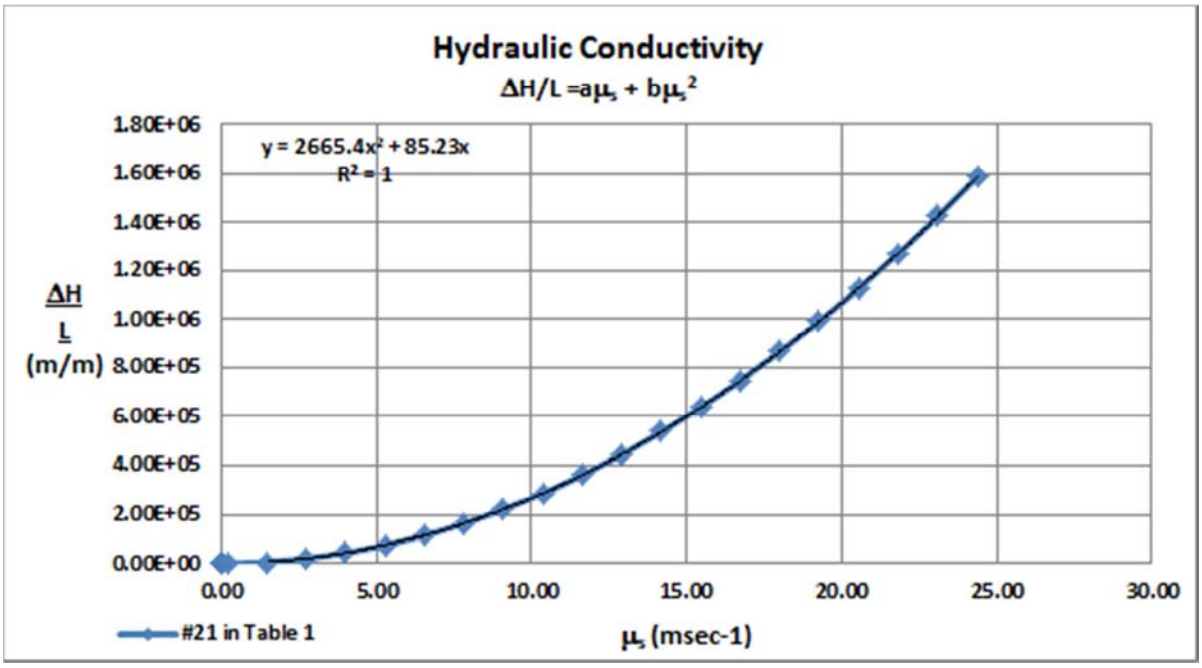

Figure 1. *Hydraulic conductivity as a quadratic function of fluid flux.*

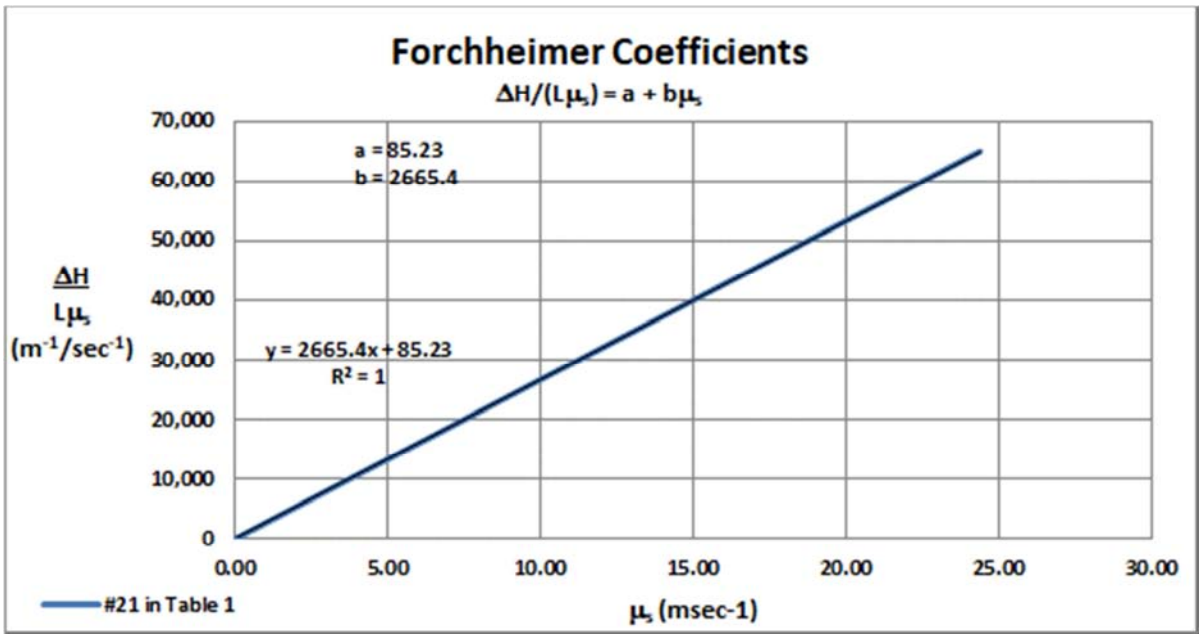

Figure 2. *Normalized hydraulic conductivity as a linear function of fluid flux.*

As shown in Figure 1, the second order polynomial trend line associated with this plot renders the values of a, and b, both of which are represented as having a constant value, over all flow rate ranges.

Alternatively, equation (4) is often used by practitioners, since a linear trend line of this plot of normalized hydraulic conductivity versus fluid flux μ_s, will render a straight line whose intercept represents the value of a, and whose slope represents the value of b, as shown in Figure 2.

As shown in Figure 2, this technique also generates a constant value for both coefficients.

2.1. Quinn's Law of Fluid Dynamics

Since Quinn's Law is universal, it applies to all fluid flow regimes. Specifically, it provides a detailed analytical definition of the fluid flow parameters which make up the numerical values of a, and b, for any experiment under study. Thus, we provide, herein, the definition for a, and b, as taught by Quinn's Law:

$$a = \frac{4r_h^3\pi\delta\eta}{3\rho_f g d_c^2} \tag{5}$$

$$b = \frac{\delta^2\lambda}{2\pi g d_c} \tag{6}$$

In addition, Quinn's Law also provides all the needed relationships between the measurable fluid flow embodiment parameters necessary to completely establish the fluid flow relationship. Thus, we include some additional pertinent equations from Quinn's law:

$$\delta = \frac{1}{\varepsilon_0^3} \tag{7}$$

$$\varepsilon_0 = 1 - \frac{n_p}{n_{pq}} = 1 - \frac{2n_p d_p^3}{3D^2L} \tag{8}$$

$$n_{pq} = \frac{3D^2L}{2d_p^3} \tag{9}$$

$$d_c = \frac{d_p}{abs(1-\varepsilon_0)} \tag{10}$$

$$\lambda=(1+W_N) \tag{11}$$

where, r_h=fluid drag normalization coefficient, i.e., 4, η=the fluid absolute viscosity, d_p=the spherical particle diameter equivalent, d_c=the diameter of the hypothetical Q-channel, n_p=the number of particles in the packed conduit under study, and λ=the normalization coefficient for wall effects, generally equal to unity for packed conduits.

Since the parameter λ, however, involves a very complex definition involving many different independent and dependent variables, we refer the reader to the original publication of Quinn's Law for all the details concerning the components of λ [48]. Additionally, for the reader's convenience, we have included in the addendum to this paper, a comprehensive reference guide which provides, nomenclature, glossary of terms and all formulae from the original publication of Quinn's Law.

2.2. Solving the Navier-Stokes Equation for Closed Conduits

Quinn's Law is the only extant theory of fluid dynamics which includes an equation capable of describing the relationship between fluid flow rate and pressure drop that is unique in its ability to describe, accurately and precisely, this relationship throughout the entire fluid flow regime, including all three so-called regions of laminar, transitional and fully turbulent. We shall now explore in detail how this is accomplished.

1. Definition of Parameters.

Quinn's Law teaches that there are 17 important parameters in the pressure flow relationship in closed conduits, representing 3 distinct categories which include: (a) constants, (b) independent variables and (c) dependent variables:

a. There are 4 constants:
   π, r_h, k_1 and k_2
b. There are 9 independent variables:

3 Fluid variables: η, ρ_f and q.
4 Packed conduit variables: D, L, n_p, and k.
2 Particle variables: d_{pm}, Ω_p,

c. There are 4 dependent variables:

1 Fluid variable: $\lambda=f(\pi, r_h, R_{em}, k, \delta,)$
3 Packed conduit variables: $d_p=f(d_{pm}, \Omega_p)$,

$$\varepsilon_0=f(\pi, D, L, d_p),$$

$$\Delta P=f(\lambda)$$

2. Formula

The formula $P_Q=k_1 + k_2C_Q$, which is the dimensionless manifestation of Quinn's Law, is a unique formula which combines the above identified variables in a manner never before contemplated.

3. Underlying theory

The theory which underpins Quinn's Law is vitally important in executing the solution to the Navier-Stokes relationship, because of the important insights derived based upon an understanding of the boundary conditions embedded within the theory.

Accordingly, what makes Quinn's Law unique is that it contains many parameters not identified in other fluid dynamic models, i.e., r_h, k_1, k_2, β_0, τ, λ, Q_N, C_Q, etc., etc., and, in addition, combines all the parameters in a unique arrangement not heretofore available in any other fluid model.

Thus, when the fluid flow rate, pressure drop and conduit diameter are determined by experiment and, accordingly, the Forchheimer values of a, and b, are known, based upon accurate measurements of these three variables over a broad range of flow rates, including the non-linear region, where kinetic contributions to measured pressure drop are significant and, in combination with the fluid property of kinematic viscosity, we can solve the N-S equation using Quinn's Law. Thus, we proceed as follows:

It follows from equation (5) above that we may write:

$$\frac{\delta}{d_c^2} = \frac{3a\rho_f g}{4r_h^3 \pi \eta} \quad (12)$$

Similarly, it follows from equation (6) above that we may write:

$$\frac{\delta^2}{d_c} = \frac{2b\pi g}{\lambda} \quad (13)$$

Therefore, in order to solve the N-S equation we must satisfy both equations (12) and (13) *simultaneously*.

From equation (12), let us assume that:

$$\frac{\delta}{d_c^2} = \alpha \quad (14)$$

From equation (13), let us assume that:

$$\frac{\delta^2}{d_c} = \beta \quad (15)$$

Let us further assume that:

$$x=\alpha\beta \quad (16)$$

Similarly, let us assume that:

$$y = \frac{\alpha}{\beta} \quad (17)$$

It follows that we may now write the solution to the N-S equation for closed conduits as:

$$d_c = \frac{1}{X^{(1/6)} y^{(1/2)}} \quad (18)$$

$$\delta = \frac{X^{(1/6)}}{y^{(1/2)}} \quad (19)$$

The above simultaneous solution for the values of d_c and δ depends, not only, upon the independent variables identified above, but also, upon the value of λ in equation (13). However, λ, in turn, depends upon the value of other variables including d_c, a dependent variable itself and, accordingly, and problematically, this is the conundrum of solving the N-S equation. Furthermore, the variable ε_0 (conduit external porosity), is clearly the most important variable amongst all the variables in the pressure flow relationship, since it appears in both the Forchheimer coefficients a, and b (equations (5 and (6)), and is also present in equations (18) and (19). *Additionally, there is no more sensitive relationship in all of physics between the value of ε_0 in the Forchheimer coefficient b, and the value of the pressure gradient $\Delta P/L$, when the fluid flow profile contains significant kinetic contributions.*

Therefore, Quinn's Law is the only fluid flow model in existence today that can return a valid analytical solution, based upon pressure drop and flow rate measurements, for the values of d_c and δ, simultaneously, for any given flow rate, in any given experiment, in a closed conduit, regardless of whether that conduit is packed with particles or empty, and regardless of where in the fluid flow regime that flow rate may fall, laminar, transitional or fully turbulent. This unequivocal assertion is a manifestation of the solution to the N-S equation for fluid flow in closed conduits.

2.3. Executing the Navier-Stokes Solution Using Quinn's Law

The theoretical basis of Quinn's Law, i.e. the Quinn Fluid Flow Model (QFFM), however, provides the means by which one can overcome this conundrum in solving the N-S equation for closed conduits, by establishing an understanding of the value of λ under three distinct closed conduit milieus, two of which are self-evident, based upon the underlying theory, and one of which necessitates an additional measurement of an independent variable.

We digress here to emphasize that the parameter λ, as defined in the QFFM, is bounded on the lower side by an asymptote which tends to the value of unity when the packed conduit tortuosity term, tau, is very large. The definition of the conduit tortuosity term tau, in turn, is based upon the architectural makeup of the particular closed conduit under study. It is, therefore, a totally novel concept for this parameter, amongst all other existing and competing theories of fluid dynamics. Consequently, the concept of conduit tortuosity, as defined in the QFFM, is what differentiates the fluid dynamics within different closed conduits and, accordingly, defines the three distinct closed conduit milieus regarding the values of λ which arise in the case of fluid flow in packed and empty closed conduits. These distinct milieus may be catalogued as follows:

1) Packed conduit with low value of the ratio D/d_p

The most general case of a packed conduit is when the ratio of D/d_p is low, say less than 10. In this scenario, Quinn's Law teaches that there is a significant primary wall effect at very low values of the modified Reynolds number and, consequently, the value of λ will not be exactly equal to 1.0 and, together with the value of the Forchheimer coefficient b, will vary based upon the fluid velocity used in any experiment under study.

It is important to understand, however, that in this milieu, even though the primary wall effect is significant at very low values of the modified Reynolds number, it will only manifest in the pressure gradient measurements at moderate values of the modified Reynolds number. This is because all wall effects, and therefore the λ parameter, manifests only in the kinetic term of Quinn's Law, which has a relatively small contribution to the measured pressure gradient at very low values of the modified Reynolds number. One could, theoretically, make measurements at very high modified Reynolds number values, where the value of λ would tend to unity as the boundary layer is dissipated, but this could require large pressure drops, not practical in a typical practitioner's laboratory. Therefore, alternatively, one must know, in addition to the values of the Forchheimer coefficients a, and b, at least one more independent variable, to solve the N-S equation in this milieu scenario at reasonable pressure drops. That independent

variable is n_p, the number of particles in any packed conduit under study, which must be independently measured in this scenario of a packed conduit. Again, we point out that in this scenario, the plotting techniques using equation (3) and (4) will not produce accurate values for the Forchheimer coefficients a, and b.

Thus, Quinn's Law is the only fluid flow model capable of validating the accuracy and precision of the underlying conduit variables of d_p, and ε_0, based upon Forchheimer type measurements of fluid flux and hydraulic conductivity, and which also include an independent measurement of the value of n_p, in this milieu, where the primary wall effect is significant at low to moderate flow rates.

2) Packed conduit with large value of the ratio D/d_p

A packed conduit where the ratio of D/d_p is large, say greater than 30. This represents a special boundary condition in the application of our solution. In this scenario, the QFFM teaches that there is no wall effect of any kind, either primary or secondary, and, consequently, because the value of the packed conduit tortuosity term, $\tau=\delta\gamma$, is very large, the value of $\lambda \rightarrow 1$, at all fluid velocities across the fluid flow regime, i.e. all values of the modified Reynolds number, R_{em}. Accordingly, the measured values for the Forchheimer coefficients a, and b, will both be constant at all fluid velocities. Thus, the above solution for the values d_c and δ is absolute at a value of $\lambda=1$, since in equation (13), all the values of the parameters are uniquely defined at this boundary condition. This is typically the case for most commercially available packed conduits, since they are typically designed with large ratios of D/d_p for performance related reasons. In this scenario, the technique outlined above of identifying the values of the Forchheimer coefficients a, and b, by plotting equations (3) and (4) will yield accurate values across the full spectrum of modified Reynolds number, if sufficient flow rate measurements are taken both in the linear and non-linear regions of the flow regime, which includes the region in which kinetic contributions to the measured pressure drop are significant. Thus, in this new teaching, measurements which include kinetic contributions are critical to identify an accurate value of the Forchheimer coefficients a, and b, regardless of what flow regime a particular experimental protocol may be focused, i.e., permeability studies in the laminar regime are included in this qualification.

We emphasize that in the literature for packed conduits in many applications, and especially in the field of chromatography, kinetic contributions to measured pressure drop have been totally ignored in favor of just doing measurements in the laminar regime. This results in inaccurate values for the Forchheimer coefficients a, and b, which, in turn, means that studies carried out under this set of experimental protocols will not facilitate validation of any underlying packed conduit variables. Indeed, when other fluid flow models are used in this scenario, such as the popular Kozeny-Carman model, in the case of packed conduits containing solid particles, and the Hagen-Poiseuille model, in the case of empty conduits, to back-calculate either the value of D, d_p or ε_0, they will provide only crude estimates of the true value of these parameters.

3) Empty conduits

All empty conduits regardless of the independent variable values which define them, i.e., the conduit diameter, D, the conduit length L, or the inner conduit wall roughness k, represent another special case of a packed conduit in the QFFM. Thus, although Quinn's Law teaches that an empty conduit has a relatively low tortuosity value and, consequently, a large value for λ at low flow rates, this is offset by the fact that its value is always constant, i.e. $\tau=3/16$, which is a consequence of *four limiting boundary* conditions for an empty conduit: (a) $d_p=D$, (b) $\delta=1/8$, (c) $n_p=-n_{pq}$, and (d) $\varepsilon_p=1$, where ε_p represents the *particle* porosity (not to be confused with ε_i, the *conduit* internal porosity), and when its value is unity, as in the case of an empty conduit, represents particles of free space. Thus, in an empty conduit, which corresponds to a packed conduit filled with particles of free space, there is less degree of freedom than in a packed conduit filled with particles which have a solid skeleton. This boundary condition, in turn, results from the Laws of Nature which dictate that solid matter and free space are mutually exclusive. It follows, therefore, that the values of λ, d_c, δ in equation (13) will be uniquely defined when these four boundary conditions prevail. Thus, setting four boundary conditions in Quinn's Law for the values of $\delta=1/8$, $d_p=D$, $n_p=-n_{pq}$ and $\varepsilon_p=1$, establishes a unique value for λ at any given flow rate, when the Forchheimer type coefficients a, and b, are known. We emphasize, however, that the technique outlined above of using plots of equations (3) and (4), as shown in Figures 1 and 2, will not produce accurate values for the Forchheimer coefficients a, and b, in the case of an empty conduit, since they are only capable of returning an average value for these coefficients and, of course, the value of b in an empty conduit varies as a function of flow rate.

Thus, Quinn's Law is the only fluid flow model capable of validating the accuracy and precision of the underlying conduit variables of D, L, and k, in an empty conduit, based upon Forchheimer type measurements of fluid flux and hydraulic conductivity.

We digress, once again, to explain the significance of Quinn's Law as it pertains to the independent variable, k, the roughness of the inner conduit wall in an empty conduit. There are just three measureable variables for an empty conduit, D, L, and k. The former two variables are easy to measure and, in addition, can usually be measured with a high degree of accuracy. This is not the case with the latter variable, k which is very difficult to measure, in the first instance, not to mention the accuracy of the measurement. Accordingly, in the case of an empty conduit, one can use the Forchheimer equivalent type measurements for an empty conduit, in conjunction with Quinn's Law, to accurately back-calculate for the value of k, when the measured data contains pressure drop measurements taken at sufficiently high values of the modified Reynolds number, where the secondary wall effect, i.e., the wall roughness coefficient, manifests itself by punching through the ever- dissipating

boundary layer. *This is a very effective tool for the practitioner.*

3. Illustrative Examples

We shall now present illustrative examples for all of the categories above as well as an example for roughened walls.

Example 1.

Our first illustrative example is based upon our own laboratory experiment involving a conduit of dimensions 0.3681 x 97.75 cm into which we packed 297 stainless steel ball bearings with a value of d_p=0.3291 cm, to which we have given the identification label of HMQ-14. [49]. In our Figure 3 below, we have included the results of our procedure for determining the values of the underlying packed conduit variables, in this case a packed conduit with a low value of D/d_p=1.12.

Mat'l Type	A	B	R_{em}	a	b	λ	dc $\frac{1}{X^{(1/6)}y^{(1/2)}}$	δ $\frac{X^{1/6}}{100Y^{1/2}}$	ε_0 $\frac{1}{\delta^{(1/3)}}$	dp $d_c abs(1-\varepsilon_0)$	n_p $\frac{3D^2L(1-\varepsilon_0)}{2d_p^3}$
			none	sm^{-1}	s^2m^{-2}		cm	none	none	cm	
Packed conduit	268.19	1.61	532	7.04	260.83	1.03	0.6175	9.8180	0.4670	0.3291	297
Dimensions	268.19	1.61	667	7.04	260.39	1.03	0.6175	9.8180	0.4670	0.3291	297
.3681 x 97.75 cm	268.19	1.60	802	7.04	260.04	1.03	0.6175	9.8180	0.4670	0.3291	297
	268.19	1.60	928	7.04	259.76	1.03	0.6175	9.8180	0.4670	0.3291	297
	268.19	1.60	1,054	7.04	259.53	1.03	0.6175	9.8180	0.4670	0.3291	297
	268.19	1.60	1,208	7.04	259.28	1.02	0.6175	9.8180	0.4670	0.3291	297
	268.19	1.60	1,315	7.04	259.13	1.02	0.6175	9.8180	0.4670	0.3291	297
	268.19	1.60	1,450	7.04	258.96	1.02	0.6175	9.8180	0.4670	0.3291	297
	268.19	1.60	1,576	7.04	258.82	1.02	0.6175	9.8180	0.4670	0.3291	297
	268.19	1.60	1,692	7.04	258.70	1.02	0.6175	9.8180	0.4670	0.3291	297
	268.19	1.60	1,817	7.04	258.58	1.02	0.6175	9.8180	0.4670	0.3291	297
	268.19	1.59	2,132	7.04	258.32	1.02	0.6175	9.8180	0.4670	0.3291	297
	268.19	1.59	2,049	7.04	258.38	1.02	0.6175	9.8180	0.4670	0.3291	297
	268.19	1.59	2,175	7.04	258.29	1.02	0.6175	9.8180	0.4670	0.3291	297
	268.19	1.59	2,301	7.04	258.20	1.02	0.6175	9.8180	0.4670	0.3291	297
	268.19	1.59	2,417	7.04	258.12	1.02	0.6175	9.8180	0.4670	0.3291	297
	268.19	1.59	2,562	7.04	258.03	1.02	0.6175	9.8180	0.4670	0.3291	297
	268.19	1.59	2,707	7.04	257.95	1.02	0.6175	9.8180	0.4670	0.3291	297
	268.19	1.59	2,833	7.04	257.88	1.02	0.6175	9.8180	0.4670	0.3291	297
	268.19	1.59	2,929	7.04	257.83	1.02	0.6175	9.8180	0.4670	0.3291	297
	268.19	1.59	3,045	7.04	257.77	1.02	0.6175	9.8180	0.4670	0.3291	297
	268.19	1.59	3,142	7.04	257.73	1.02	0.6175	9.8180	0.4670	0.3291	297
	268.19	1.59	3,287	7.04	257.66	1.02	0.6175	9.8180	0.4670	0.3291	297
	268.19	1.59	3,384	7.04	257.62	1.02	0.6175	9.8180	0.4670	0.3291	297
	268.19	1.59	3,577	7.04	257.54	1.02	0.6175	9.8180	0.4670	0.3291	297
	268.19	1.59	3,625	7.04	257.52	1.02	0.6175	9.8180	0.4670	0.3291	297
	268.19	1.59	3,722	7.04	257.49	1.02	0.6175	9.8180	0.4670	0.3291	297

Figure 3. *Packed conduit with low value for D/d_p.*

As shown in Figure 3, the value of λ is greater than 1 at low flow rates and gradually decreases in value with increasing flow rate. The value for the Q-modified Ergun coefficient A, on the other hand, is constant at a value of 268.19, but the value of B varies between 1.61 and 1.59 over the range of modified Reynolds number values of 500 to 4,000 approx. Similarly, the value of the Forchheimer coefficient a, is constant at 7.04 but the value of b, steadily decreases from 261 to 257 approx.

In our Figure 4 below, we show the inaccurate Forchheimer coefficient values for a, and b, generated by the procedure of making plots after equations (3) and (4).

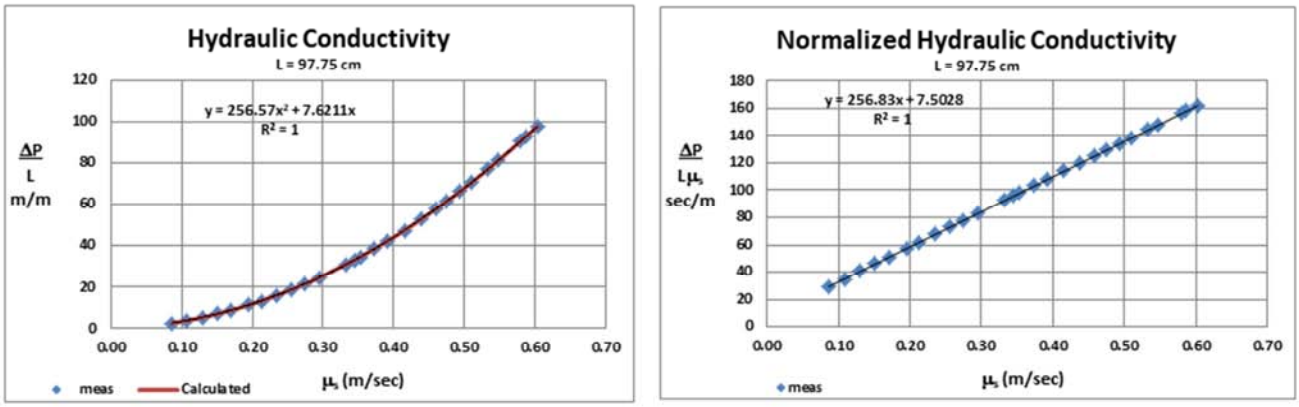

Figure 4. *Packed conduit with low D/d_p ratio data plotted after equations (3) and (4).*

As can be seen in Figure 4, neither of the plotted graphs generate the correct Forchheimer coefficient values for a, and b, and, in addition, each plot generates a constant value for each coefficient but with slightly *different* magnitudes.

Finally, in our Figure 5 below, based upon the teaching of Quinn's Law, we show a complete picture of the performance characteristics of this packed conduit over the corresponding flow rate range of 55 to 385 mL/min.

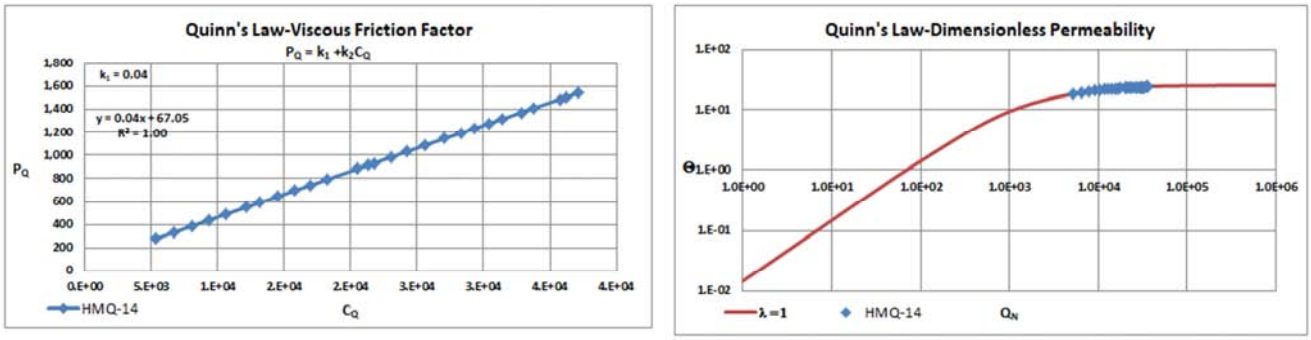

Figure 5. *Performance characteristics of packed conduit with low value for D/d_p ratio.*

We emphasize here that in the plot of dimensionless permeability in Figure 5, the measured values appear to overlay the line for $\lambda=1$. This is because we typically show this plot as a log-log plot. If, on the other hand, we simply focused on the narrow range of Q_N values measured in this example, and used linear coordinates, we would see that the measured values are offset slightly from the line for $\lambda=1$. We offer this as a cautionary note to the reader because in many instances in the published literature, and especially in this field of study relative to the scaling of experiments over a very broad range of modified Reynolds number values, unscrupulous authors have used log-log plots to hide empirical evidence which does not otherwise support their theoretical narratives.

Example 2.

Our second illustrative example is taken from a paper by Sidiropouloe, et al., published in 2007 [50]. In that paper, the authors present empirical data for 115 different packed conduits with many different types of particles.

It is noteworthy to point out, initially, that in samples numbered 1 through 26 in the paper, there are no values provided for the Forchheimer coefficient b. Accordingly, it is apparent that for these samples, the authors totally ignored kinetic contributions and, consequently, as pointed out above, their reported values for the underlying packed conduit variables cannot be validated based upon this empirical evidence.

In our Figure 6 below, we have selected some of the samples from their paper in which the authors reported both Forchheimer coefficient values for a, and b. In addition, we note that in our subset of reported samples, there is only a constant value reported for both coefficients. Accordingly, we assume that the ratio of D/d_p was large in all cases, a *critical experimental detail* which we could not find emphasized anywhere in the paper. As shown in our Figure 6, we have included the results of our procedure for determining the values of the underlying packed conduit variables. Furthermore, we have included a comparison between our calculated values for the external porosity, ε_0, and the values reported by the authors. As shown in the figure, there are some very significant differences for the values of this variable which we attribute to the experimental methodology used by the authors to measure the value of the external porosity, ε_0, and/or the particle diameter equivalent, d_p, neither of which, we contend, was sufficiently accurate or precise. These discrepancies are symptomatic of the typical experimental protocols used in the engineering disciplines regarding fluid flow through packed conduits.

Mat'l Type	Sample No.	A	B	R_{em}	a	b	λ	dc $\frac{1}{X^{(1/6)}Y^{(1/2)}}$	δ $\frac{X^{1/6}}{100Y^{1/2}}$	ε_0 $\frac{1}{\delta^{(1/3)}}$	dp $d_c abs(1-\varepsilon_0)$	n_p $\frac{3D^2L(1-\varepsilon_0)}{2d_p^3}$	ε_0 reported	Δ%
				none	sm^{-1}	s^2m^{-2}		cm	none	none	cm			
Sand	21	268.19	3.27	0.002	85.23	2,665	1.00	0.2567	20.5391	0.3652	0.1629	2.20E+05	0.399	8%
Sand	21	268.19	3.27	0.049	85.23	2,665	1.00	0.2567	20.5391	0.3652	0.1629	2.20E+05	0.399	8%
Sand	22	268.19	3.54	0.001	95.18	3,182	1.00	0.2530	22.2778	0.3554	0.1631	2.23E+05	0.391	9%
Angular Gravel	23	268.19	5.25	0.014	8.80	1,745	1.00	1.0126	33.0057	0.3117	0.6969	5.61E+03	0.467	33%
Angular Gravel	24	268.19	6.83	0.014	11.98	3,018	1.00	0.9896	42.9151	0.2856	0.7070	6.15E+03	0.47	39%
Angular Gravel	25	268.19	11.79	0.007	1.16	2,130	1.00	4.1790	74.0883	0.2381	3.1840	3.82E+03	0.465	49%
Angular Gravel	26	268.19	6.87	0.008	2.96	1,516	1.00	1.9977	43.2094	0.2850	1.4284	6.76E+03	0.461	38%
Sand	27	268.19	3.08	35.318	99.00	2,630	1.00	0.2313	19.3654	0.3724	0.1451	3.08E+05	0.4	7%
Sand	28	268.19	3.51	27.115	115.00	3,450	1.00	0.2291	22.0753	0.3565	0.1474	3.01E+05	0.381	6%
Sand	29	268.19	2.50	42.099	32.50	1,101	1.00	0.3635	15.7073	0.3993	0.2183	8.66E+04	0.436	8%
Sand	29	268.19	2.51	0.069	32.50	1101	1.00	0.3635	15.7073	0.3993	0.2183	8.66E+04	0.436	9%
Sand	30	268.19	3.27	28.444	47.50	1,990	1.00	0.3438	20.5401	0.3651	0.2183	9.16E+04	0.417	12%
Sand	31	268.19	3.04	31.742	40.00	1,639	1.00	0.3615	19.1157	0.3740	0.2263	8.11E+04	0.403	7%
Sand	32	268.19	2.52	34.815	13.50	720	1.00	0.5668	15.8625	0.3980	0.3412	3.27E+04	0.43	7%
Sand	33	268.19	2.43	34.015	22.50	880	1.00	0.4311	15.2933	0.4029	0.2574	5.25E+04	0.423	5%
Sand	34	268.19	2.50	40.313	7.50	530	1.00	0.7571	15.7251	0.3991	0.4549	1.88E+04	0.384	-4%
Sand	35	268.19	2.89	38.538	10.50	780	1.00	0.6882	18.1893	0.3802	0.4265	2.70E+04	0.367	-4%
Gravel	36	268.19	2.62	44.504	4.30	430	1.00	1.0236	16.4812	0.3929	0.6214	1.03E+04	0.372	-6%
Gravel	37	268.19	2.57	33.340	7.50	550	1.00	0.7669	16.1332	0.3958	0.4634	2.48E+04	0.356	-11%
Gravel	38	268.19	2.89	29.920	10.50	780	1.00	0.6882	18.1908	0.3802	0.4265	3.26E+04	0.346	-10%
Round river gra	39	268.19	3.08	35.263	99.00	2,630	1.00	0.2313	19.3655	0.3724	0.1451	2.83E+04	0.4	7%
Round river gra	40	268.19	3.51	26.995	115.00	3,450	1.00	0.2291	22.0775	0.3565	0.1474	2.77E+04	0.381	6%
Round river gra	41	268.19	2.50	42.680	32.50	1,100	1.00	0.3634	15.7020	0.3993	0.2183	2.25E+04	0.436	8%
Round river gra	42	268.19	3.27	28.601	47.50	1,990	1.00	0.3438	20.5398	0.3651	0.2183	2.38E+04	0.417	12%
Round river gra	43	268.19	3.04	31.839	40.00	1,640	1.00	0.3615	19.1197	0.3740	0.2263	2.11E+04	0.403	7%
Round river gra	44	268.19	4.48	19.872	51.50	3,330	1.00	0.3868	28.1807	0.3286	0.2597	1.50E+04	0.392	16%
Round river gra	45	268.19	2.52	36.257	13.50	720	1.00	0.5668	15.8643	0.3980	0.3412	1.67E+04	0.43	7%
Round river gra	46	268.19	2.43	33.536	22.50	880	1.00	0.4311	15.2930	0.4029	0.2574	3.87E+04	0.423	5%
Round river gra	47	268.19	1.25	73.967	34.00	400	1.00	0.2517	7.8770	0.5026	0.1252	2.80E+05	0.403	-25%
Round river gra	48	268.19	2.50	42.639	7.50	530	1.00	0.7571	15.7239	0.3992	0.4549	1.41E+04	0.384	-4%
Round river gra	49	268.19	2.89	38.759	10.50	780	1.00	0.6882	18.1919	0.3802	0.4265	1.76E+04	0.367	-4%
Round river gra	50	268.19	2.62	44.505	4.30	430	1.00	1.0237	16.4797	0.3930	0.6214	1.03E+04	0.372	-6%
Round river gra	51	268.19	2.57	33.341	7.50	550	1.00	0.7669	16.1346	0.3957	0.4634	2.48E+04	0.356	-11%
Round river gra	52	268.19	2.89	29.919	10.50	780	1.00	0.6882	18.1889	0.3802	0.4265	3.26E+04	0.346	-10%
Crushed Rock	93	268.19	2.19	0.002	35.15	940	1.00	0.3273	13.7774	0.4171	0.1908	1.26E+05	0.42	1%
Crushed Rock	94	268.19	2.44	0.000	1.90	258	1.00	1.4870	15.3680	0.4022	0.8889	2.04E+04	0.43	6%
Crushed Rock	95	268.19	1.35	0.000	2.25	115	1.00	1.0163	8.5038	0.4899	0.5184	8.79E+04	0.415	-18%
Glass Spheres	96	268.19	0.75	0.000	2.03	45	1.00	0.7943	4.6844	0.5977	0.3196	6.66E+05	0.383	-56%
Glass Spheres	97	268.19	0.59	0.000	1.53	27	1.00	0.8148	3.7158	0.6456	0.2888	2.21E+06	0.392	-65%
Crushed Rock	98	268.19	0.98	0.000	0.38	29	1.00	2.1054	6.1591	0.5455	0.9568	2.80E+04	0.466	-17%
Crushed Rock	99	268.19	2.53	0.000	2.40	304	1.00	1.3456	15.8921	0.3977	0.8104	6.11E+04	0.472	16%
Crushed Rock	100	268.19	10.24	0.001	0.64	1,280	1.00	5.2463	64.3407	0.2496	3.9370	6.64E+02	0.445	44%
Crushed Rock	101	268.19	2.45	0.000	1.25	210	1.00	1.8371	15.4227	0.4017	1.0991	2.43E+04	0.441	9%
Crushed Rock	102	268.19	1.76	0.000	1.13	122	1.00	1.6375	11.0815	0.4485	0.9030	4.04E+04	0.444	-1%
Crushed Rock	103	268.19	1.90	0.000	0.72	108	1.00	2.1285	11.9318	0.4376	1.1970	1.77E+04	0.373	-17%
Round gravel	104	268.19	1.44	0.000	6.03	207	1.00	0.6403	9.0442	0.4800	0.3330	7.60E+05	0.357	-34%
Round gravel	105	268.19	1.37	0.000	5.63	187	1.00	0.6474	8.6316	0.4875	0.3318	7.58E+05	0.479	-2%
Angular gravel	106	268.19	1.38	0.000	2.71	130.16	1.00	0.9349	8.6623	0.4869	0.4797	2.51E+05	0.479	-2%
Crushed Rock	107	268.19	0.75	0.000	4.45	67	1.00	0.5385	4.7198	0.5962	0.2175	2.12E+06	0.47	-27%
Glass Spheres	108	268.19	1.16	0.000	1.20	67	1.00	1.2877	7.2780	0.5160	0.6232	1.08E+05	0.395	-31%
Glass Spheres	109	268.19	1.01	0.000	1.25	56	1.00	1.1794	6.3595	0.5397	0.5428	1.55E+05	0.382	-41%
Crushed Rock	110	268.19	0.95	0.000	1.55	57	1.00	1.0283	5.9962	0.5504	0.4623	2.46E+05	0.458	-20%
Glass Spheres	111	268.19	0.80	0.000	0.60	27	1.00	1.5099	5.0040	0.5846	0.6271	2.05E+05	0.413	-42%
Crushed Rock	112	268.19	0.72	0.000	1.10	31	1.00	1.0602	4.5217	0.6047	0.4191	6.53E+05	0.487	-24%
Glass Spheres	113	268.19	1.41	0.000	1.42	98	1.00	1.3083	8.8891	0.4827	0.6767	9.01E+04	0.355	-36%
Glass Spheres	114	268.19	2.26	0.000	0.76	145	1.00	2.2591	14.1908	0.4130	1.3260	1.36E+04	0.355	-16%
Glass Spheres	115	268.19	1.26	0.000	0.31	38.6	1.00	2.6465	7.9393	0.5013	1.3199	2.64E+04	0.398	-26%

Figure 6. *Packed conduit with high value for D/d_p ratio.*

In our Figure 7 below, for illustration purposes, using the teaching of Quinn's Law, we show a complete picture of the performance characteristics of sample number 21from this paper over a modified Reynolds number range value of 1 to 70,00.

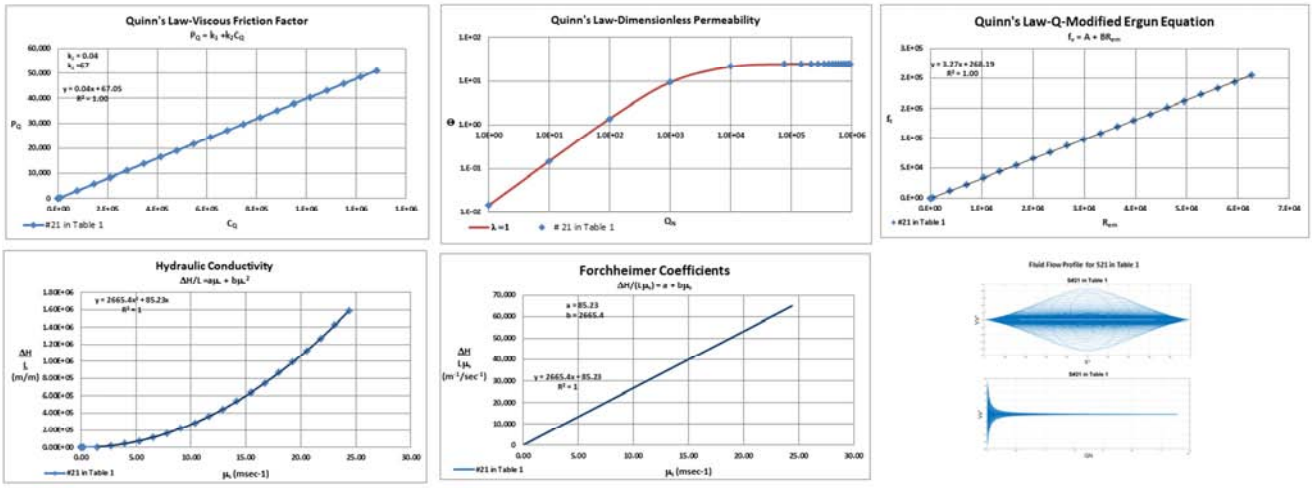

Figure 7. *Performance Characteristics of sample no. 21.*

Example 3.

Our third illustrative example is based upon our own laboratory experiment involving a peak capillary tubing of nominal dimensions 0.02 inches in diameter and 12 inches in length [51]. In our Figure 8 below, we have included the results of our procedure for determining the values of the underlying packed conduit variables, in this case an empty capillary. In addition, in our Figure 9 below, using the teaching of Quinn's Law, we show a complete picture of the performance characteristics of this empty conduit over a flow rate range of 20 to 125 mL/min.

Mat'l Type	A	B	R_{em}	a	b	λ	dc	δ	ε_0	dp	n_p
							$\frac{1}{X^{(1/6)}Y^{(1/2)}}$	$\frac{X^{1/6}}{100Y^{1/2}}$	$\frac{1}{\delta^{(1/3)}}$	$d_c abs(1-\varepsilon_0)$	$\frac{3D^2L(1-\varepsilon_0)}{2d_p^3}$
			none	sm^{-1}	s^2m^{-2}		cm	none	none	cm	
Empty conduit type	268.19	0.12	919	13.24	3.10	6.22	0.0508	0.1250	2.0000	0.0508	-886
Peek Capillary tube	268.19	0.12	1253	13.24	3.08	6.18	0.0508	0.1250	2.0000	0.0508	-886
Nominal dimensions	268.19	0.12	1545	13.24	3.06	6.14	0.0508	0.1250	2.0000	0.0508	-886
0.02 x 12 inches	268.19	0.12	1837	13.24	3.05	6.11	0.0508	0.1250	2.0000	0.0508	-886
	268.19	0.12	2088	13.24	3.03	6.08	0.0508	0.1250	2.0000	0.0508	-886
	268.19	0.12	2464	13.24	3.01	6.04	0.0508	0.1250	2.0000	0.0508	-886
	268.19	0.12	2798	13.24	3.00	6.01	0.0508	0.1250	2.0000	0.0508	-886
	268.19	0.12	3090	13.24	2.98	5.98	0.0508	0.1250	2.0000	0.0508	-886
	268.19	0.12	3340	13.24	2.97	5.95	0.0508	0.1250	2.0000	0.0508	-886
	268.19	0.12	3591	13.24	2.96	5.93	0.0508	0.1250	2.0000	0.0508	-886
	268.19	0.12	3883	13.24	2.94	5.90	0.0508	0.1250	2.0000	0.0508	-886
	268.19	0.12	4050	13.24	2.94	5.89	0.0508	0.1250	2.0000	0.0508	-886
	268.19	0.12	4468	13.24	2.92	5.85	0.0508	0.1250	2.0000	0.0508	-886
	268.19	0.12	4718	13.24	2.91	5.83	0.0508	0.1250	2.0000	0.0508	-886
	268.19	0.12	4885	13.24	2.90	5.81	0.0508	0.1250	2.0000	0.0508	-886
	268.19	0.11	5220	13.24	2.88	5.78	0.0508	0.1250	2.0000	0.0508	-886
	268.19	0.11	5303	13.24	2.88	5.78	0.0508	0.1250	2.0000	0.0508	-886
	268.19	0.11	5637	13.24	2.87	5.75	0.0508	0.1250	2.0000	0.0508	-886
	268.19	0.11	6263	13.24	2.84	5.70	0.0508	0.1250	2.0000	0.0508	-886
	268.19	0.11	6681	13.24	2.83	5.66	0.0508	0.1250	2.0000	0.0508	-886
	268.19	0.11	7099	13.24	2.81	5.63	0.0508	0.1250	2.0000	0.0508	-886
	268.19	0.11	7516	13.24	2.79	5.60	0.0508	0.1250	2.0000	0.0508	-886
	268.19	0.11	8128	13.24	2.77	5.56	0.0508	0.1250	2.0000	0.0508	-886

Figure 8. *An empty conduit.*

As shown in Figure 8, the value of the Q-modified Ergun coefficient A, and the value of the Forchheimer coefficient a, are constant at all Reynolds number values, but the values of B, b and λ change as a function of the modified Reynolds number R_{em}. Since this capillary has a smooth inner wall, the changing values of the three parameters mentioned, i.e., B, b and λ, are due to the primary wall effect whose impact on permeability is most pronounced at modest Reynolds number values. Note that the value of λ in this scenario is relatively large, since an empty conduit has a low and *constant* value for the τ parameter.

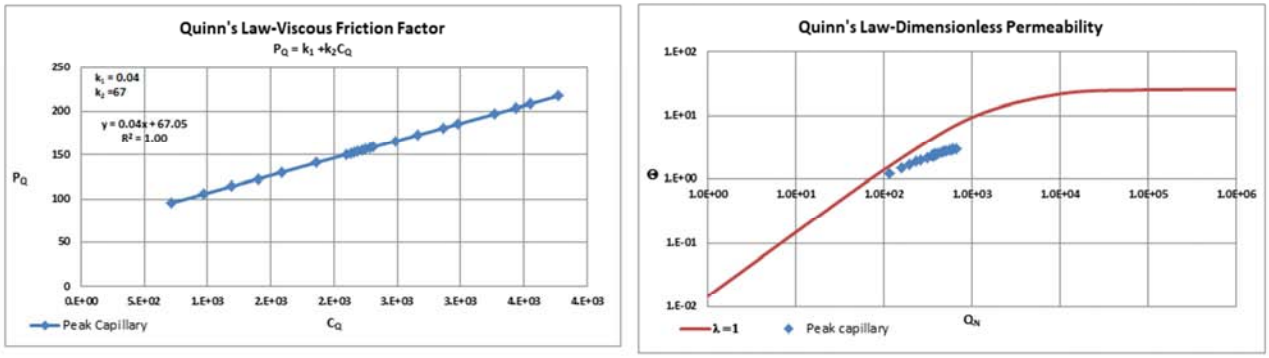

Figure 9. *Performance characteristics of an empty conduit.*

It is obvious from Figure 9, in the plot of Θ v Q_N, that in this example, the primary wall effect has a negligible impact at very low values of Q_N, i.e., it coincides with the line for λ=1, but manifests significantly through moderate values of Q_N and, if projected in a straight line in our mind's eye, would coincide once again with the line for λ=1, at very high values of Q_N. This is a manifestation of the dissipation of the boundary layer as the fluid becomes fully turbulent at high values of Q_N.

Example 4.

Our fourth illustrative example is based upon the work reported by Nikuradze [38]. This is the classical study carried out circa 1930 which involved the grafting of particles of sand onto the inner surface of drawn brass pipes to create six levels of wall roughness criteria. Even to this day, this study is considered the gold standard of wall roughness empirical data. We have plotted Nikuradze's measured data according to the teaching of Quinn's Law for dimensionless permeability in our Figure 10 below.

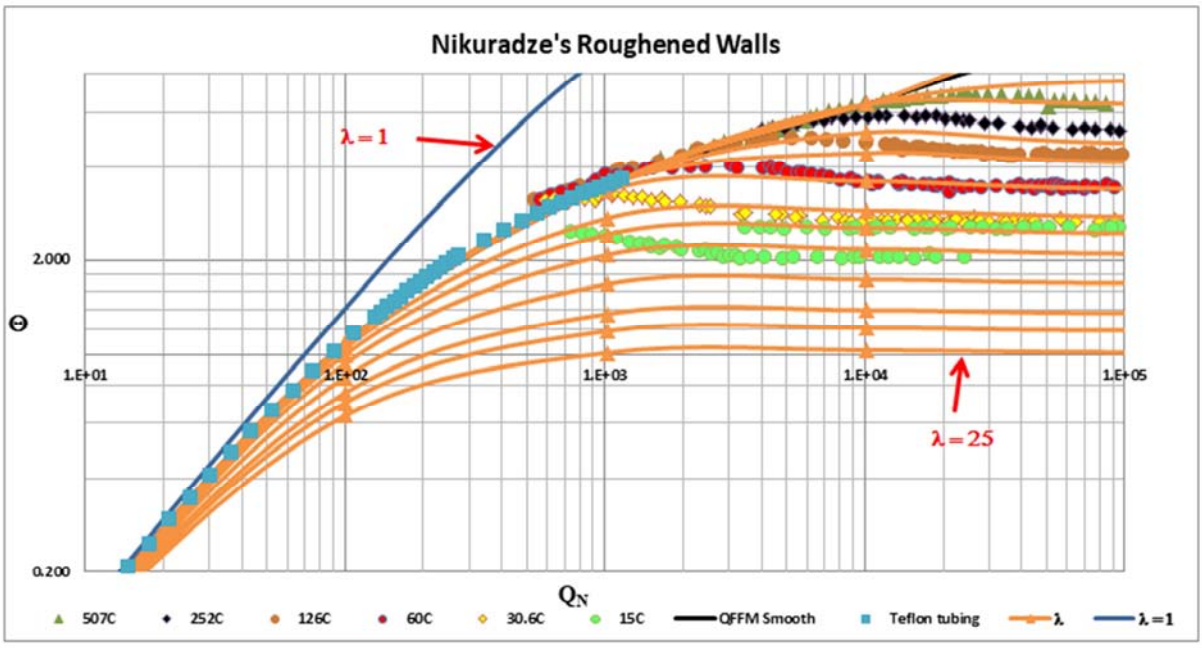

Figure 10. *Overlay of Nikuradze's roughened data.*

As shown in Figure 10, we have superimposed Nikuradze's measured results on the underlying background of the λ parameter taught in Quinn's law, in our plot of dimensionless permeability. As shown in the plot, Nikuradze's roughened data falls within a range of λ values from 2 to 11, approximately. It is obvious from the plot that the secondary wall effect, i.e., the roughness coefficient, manifests at sufficiently high modified Reynolds number values as the boundary layer is progressively dissipated, *commensurate with the magnitude of the roughness coefficient of a particular conduit under study.*

4. Evaluating Third Party Published Works

We shall now evaluate a cross-section of published articles in the literature, applying our solution to the N-S equation using the teachings of Quinn's Law, to pinpoint discrepancies which are commonplace in the literature due to inadequate measurement techniques. To highlight the discrepancies, our

analysis will generate the Q-Modified Ergun constants, A, and B, the Forchheimer coefficients, a, and b, the value of λ̣as well as our back-calculated values for the conduit variables, for each sample evaluated. For guidance in our analysis, we shall follow a precise accept/reject procedure as follows;

We shall apply the Q-modified Ergun equation as an accept/reject criteria for any reported packed conduit data having solid particles. In particular, we shall use the value for the B coefficient as our measurement standard with respect to conduit packed density, i.e., external porosity. Therefore, consistent with our own experience of packing many conduits with a variety of rigid particles (the packed conduits being numbered in the hundreds of thousands over a career of 30 plus years), which dictates that well-packed conduits have a range of external porosities of 0.36 to 0.47, and based upon the teaching of Quinn's Law for the value of the coefficient B, our accept/reject criteria for the value of B is: $1.5 < B < 3.5$. The value of B=1.5 represents the highest value of external porosity possible, i.e. ε_0=0.47, and a value of B=3.5 represents the lowest value of external porosity possible, i.e., ε_0=0.36.

Example 5: Data of Banerjee et al 2017 & 2019

In a recent published article (2019), whose title would seem to suggest that the authors had discovered something important related to permeability "Over the Complete Flow Regime", Banerjee et al claim that they have made a correlation between the Forchheimer coefficients a, and b, which dictates that the values of the coefficients are a function of the fluid flow profile [52]. In fact, they define "corrections" to several parameters in their 2017 paper and "create" a parameter which they designate as, γ, whose value changes over the fluid flow regime and suggests that both values of the Forchheimer coefficients a, and b, are a function of this γ parameter. We categorically disagree with the author's conclusions, as well as the "corrections" upon which they are based.

Firstly, the authors make it a point to present hydraulic conductivity data representing external porosity values of packed conduits ranging from 0.30 to 0.50. This range is far too broad based upon our experience of packing many conduits with various rigid particle types and, in addition, their paper lacks any meaningful analysis of the role of external porosity or the care with which they measured its value, which variable is clearly the most sensitive element impacting their reported development.

To illustrate our arguments, we have applied our N-S solution for closed conduits to a subset of the data reported in this paper and captured our analysis results in Figure 11 below.

Sample ID	A	B	a	b	λ	d_c $\frac{1}{X^{(1/6)}Y^{(1/2)}}$	δ $\frac{X^{1/6}}{Y^{1/2}}$	ε_0 $\frac{1}{\delta^{(1/3)}}$	d_p $d_c abs(1-\varepsilon_0)$	n_p $\frac{3D^2L(1-\varepsilon_0)}{2d_p^3}$	d reported	Δd %	ε_0 reported	$\Delta\varepsilon_0$ %
			sm^{-1}	s^2m^{-2}		cm	none	none	cm		cm		none	
2017														
a	268.19	0.18	0.056	3.725	1.000	3.797	2.95	0.6970	1.150	2,315	2.980	61%	0.4059	42%
Crushed stones	268.19	0.40	0.025	3.542	1.000	6.392	3.74	0.6444	2.273	2,315	2.980	24%	0.4334	33%
	268.19	0.18	0.045	3.304	1.000	4.221	2.93	0.6987	1.272	2,315	2.980	57%	0.4569	35%
b	268.19	0.16	0.083	3.444	1.000	2.845	2.46	0.7410	0.737	2,315	3.478	79%	0.4171	44%
Crushed stones	268.19	0.19	0.045	3.420	1.000	4.270	3.00	0.6933	1.309	2,315	3.478	62%	0.4470	36%
	268.19	0.16	0.068	3.025	1.000	3.112	2.41	0.7459	0.791	2,315	3.478	77%	0.4634	38%
c	268.19	0.16	0.057	2.606	1.000	3.331	2.31	0.7561	0.812	2,315	4.159	80%	0.4103	46%
Crushed stones	268.19	0.17	0.047	2.516	1.000	3.744	2.41	0.7459	0.952	2,315	4.159	77%	0.4362	42%
	268.19	0.17	0.046	2.322	1.000	3.698	2.30	0.7575	0.897	2,315	4.159	78%	0.4615	39%
2019														
a	268.19	3.71	0.3031	192.11	1.000	4.585	23.31	0.3501	2.980	1,662	2.980	0%	0.4059	-16%
Crushed stones	268.19	3.21	0.2482	139.79	1.000	4.711	20.15	0.3675	2.980	1,617	2.980	0%	0.4334	-18%
	268.19	2.70	0.1946	95.44	1.000	4.880	16.95	0.3893	2.980	1,562	2.980	0%	0.4569	-17%
b	268.19	3.25	0.1854	123.03	1.000	5.486	20.40	0.3660	3.478	1,389	3.478	0%	0.4171	-14%
Crushed stones	268.19	3.10	0.1740	111.34	1.000	5.534	19.49	0.3716	3.478	1,377	3.478	0%	0.4470	-20%
	268.19	2.95	0.1622	99.67	1.000	5.590	18.54	0.3779	3.478	1,363	3.478	0%	0.4634	-23%
c	268.19	3.72	0.1563	138.60	1.000	6.396	23.38	0.3497	4.159	1,191	4.159	0%	0.4103	-17%
Crushed stones	268.19	3.40	0.1385	114.25	1.000	6.500	21.40	0.3602	4.159	1,172	4.159	0%	0.4362	-21%
	268.19	2.75	0.1027	71.38	1.000	6.783	17.28	0.3868	4.159	1,123	4.159	0%	0.4615	-19%
e	268.19	2.73	21.96	1032.93	1.000	0.462	17.16	0.3877	0.283	16,486	0.283	0%		N/A
Sedghi-Asl et al	268.19	3.37	7.81	845.15	1.000	0.861	21.19	0.3614	0.550	8,848	0.550	0%		N/A
	268.19	2.41	1.94	255.26	1.000	1.460	15.16	0.4041	0.870	5,220	0.870	0%		N/A
	268.19	3.33	0.95	290.16	1.000	2.448	20.93	0.3629	1.560	3,112	1.560	0%		N/A
f	268.19	2.18	0.4141	101.24	1.00	3.008	13.70	0.4179	1.751	2,533	1.751	0%	0.4726	-13%
Glass Spheres	268.19	1.65	0.1282	37.06	1.00	4.703	10.37	0.4586	2.546	1,620	2.546	0%	0.5193	-13%
	268.19	1.84	0.0882	36.28	1.00	5.990	11.58	0.4421	3.342	1,272	3.342	0%	0.5401	-22%
5mm	268.19	5.89	19.85	3114.43	1.00	0.714	37.04	0.300	0.500	10,668				
	268.19	3.71	10.78	1146.87	1.00	0.769	23.32	0.350	0.500	9,906				
	268.19	2.49	6.15	475.12	1.00	0.833	15.62	0.400	0.500	9,144				
	268.19	1.75	3.63	214.83	1.00	0.909	10.97	0.450	0.500	8382				
	268.19	1.27	2.19	103.79	1.00	1.000	8.00	0.500	0.500	7620				

Figure 11. *Our analysis of Banarjee et al.*

As can be seen in Figure 11, we have assumed a D/d_p ratio of 10, for all the packed conduits in our sample set, thus eliminating all wall effects. The reported hydraulic conductivity data in this paper renders values for the Q-modified Ergun constant B which is consistent with our accept/reject criteria. It is apparent, however, that the author's values for external porosity are significantly larger (10-20%) than those generated by our application of the N-S equation using Quinn's Law. This discrepancy is at the heart of the author's methodology because, as dictated by Quinn's Law, both the Forchheimer coefficients a, and b, are very sensitive functions of this parameter as can be seen from our equations (5) and (6) above. Moreover, the coefficient b is an extremely sensitive function of the value of the external porosity, which means that any discrepancy in porosity values will produce greatly exaggerated errors in predicted values for hydraulic conductivity when kinetic contributions dominate.

In our Figure 12 below, we show the relationship dictated by Quinn's law between the values of the Forchheimer coefficients a, and b, and external porosity, for a conduit packed with 5mm spherical particles at a D/d_p ratio of 10. In this scenario, our λ value is 1.00.

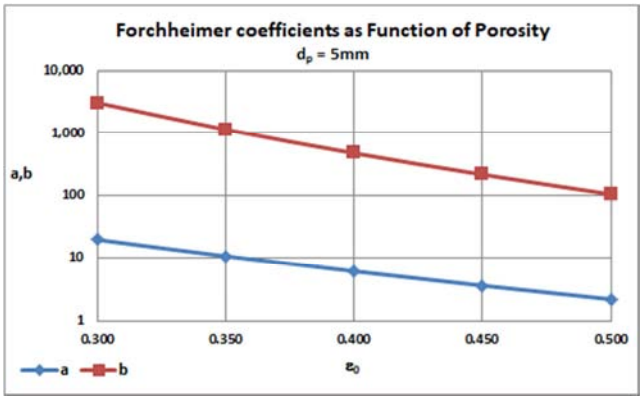

Figure 12. *Forchheimer coefficients as function of porosity.*

In Figure 13 below, we show the teaching of Quinn's law relative to hydraulic conductivity and the Forchheimer coefficients over a wide range of modified Reynolds number, for a conduit packed with 5mm spherical particles, at an external porosity of 0.30 (suggested by the paper's authors) and a D/d_p ratio of 10.

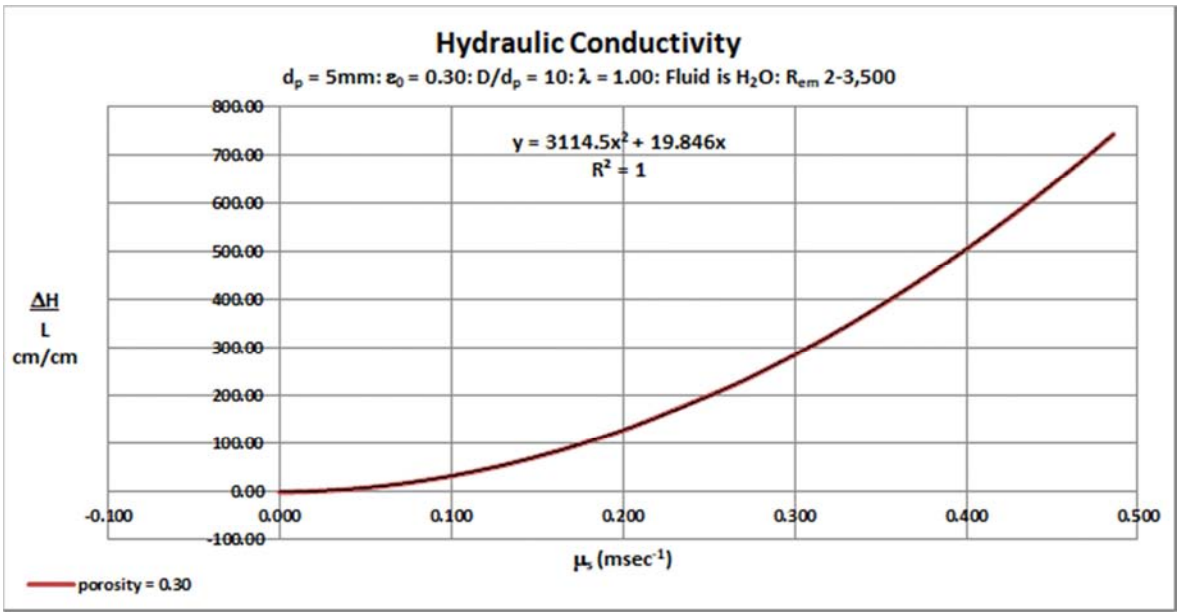

Figure 13. *Hydraulic conductivity for 5mm diameter particles.*

As can be seen from Figure 13, the values of the Forchheimer coefficients a, and b, remain constant over an extended range of modified Reynolds number values, R_{em}, i.e. 2-3,500, which represents a significantly changing fluid profile. This conclusion is at odds with the assertions made by the authors in their paper.

Finally, it is noteworthy to point out that the paper author's development is based upon the manifestly absurd assumption that "The flow path is assumed to be straight and undeviating through the porous packing". One wonders how the authors could rationalize this false assumption with their statement that they used empirical data to validate their theoretical development, since everyone knows that the flow is decidedly sinuous in conduits packed with crushed stones.

Example 6. Data of Shrinivas et al 2014

In this worked example, the authors reported on the permeability of various crushed rock [53]. The paper includes results for the "present study" as well as data by Nasser and Niranjan. In our Figure 14 below, we have captured our analysis for this data set.

Mat'l Type	Sample #	A	B	a	b	λ	d_c $\frac{1}{X^{1/\delta}Y^{1/\varepsilon}}$	δ $\frac{X^{1/\delta}}{100Y^{1/\varepsilon}}$	ε_0 $\frac{1}{\delta^{(1/3)}}$	d_p $d_c abs(1-\varepsilon_0)$	n_p $\frac{3D^2L(1-\varepsilon_0)}{2d_p^3}$	d_p reported	ε_0 reported	Δd_p%	$\Delta\varepsilon_0$%
		none	none	sm^{-1}	s^2cm^{-2}	none	cm	none	none	cm	none	cm	none	none	none
Present study															
Crushed rock	1	268.19	2.19	8.37	459	###	0.67	14	0.4171	0.3910	2.11E+06	0.325	0.4890	-20%	15%
Crushed rock	2	268.19	3.32	4.37	619	###	1.14	21	0.3631	0.7281	3.57E+05	0.473	0.4700	-54%	23%
Crushed rock	3	268.19	2.36	1.01	178	###	2.00	15	0.4070	1.1880	7.65E+04	1.000	0.4834	-19%	16%
Crushed rock	4	268.19	2.21	1.59	203	###	1.55	14	0.4158	0.9037	1.71E+05	1.164	0.4403	22%	6%
Crushed rock	**5**	**268.19**	**0.94**	**8.8**	**133**	###	**0.43**	**6**	**0.5524**	**0.1922**	**1.36E+07**	**1.310**	**0.4305**	**85%**	**-28%**
Crushed rock	**6**	**268.19**	**0.96**	**1.54**	**57**	###	**1.03**	**6**	**0.5494**	**0.4662**	**9.62E+05**	**2.010**	**0.4588**	**77%**	**-20%**
Crushed rock	**7**	**268.19**	**0.71**	**1.12**	**31**	###	**1.04**	**4**	**0.6072**	**0.4103**	**1.23E+06**	**2.890**	**0.4873**	**86%**	**-25%**
Crushed rock	**8**	**268.19**	**0.84**	**0.16**	**15**	###	**3.00**	**5**	**0.5747**	**1.2759**	**4.43E+04**	**3.950**	**0.4826**	**68%**	**-19%**
Glass spheres	9	268.19	1.52	0.49	64	###	2.31	10	0.4715	1.2195	6.30E+04	1.541	0.4181	21%	-13%
Glass spheres	**10**	**268.19**	**1.40**	**0.41**	**52**	###	**2.42**	**9**	**0.4840**	**1.2511**	**5.70E+04**	**1.803**	**0.4194**	**31%**	**-15%**
Glass spheres	**11**	**268.19**	**0.99**	**0.25**	**24**	###	**2.61**	**6**	**0.5440**	**1.1882**	**5.88E+04**	**2.837**	**0.4250**	**58%**	**-28%**
Nasser's data															
Crushed rock		**268.19**	**8.09**	**0.09**	**336**	###	**12.41**	**51**	**0.2702**	**9.0580**	**2.12E+02**	**0.690**	**0.4720**	**-1213%**	**43%**
Crushed rock		**268.19**	**6.34**	**0.03**	**133**	###	**18.96**	**39**	**0.2938**	**13.3859**	**6.37E+01**	**1.680**	**0.4450**	**-697%**	**34%**
Crushed rock		268.19	2.24	0.02	23	###	13.84	14	0.4148	8.0978	2.38E+02	4.360	0.5000	-86%	17%
Niranjan's data															
Crushed rock		268.19	2.41	28.8	980	###	0.38	15	0.4043	0.2258	1.12E+07	0.318	0.4200	29%	4%
Crushed rock		268.19	2.66	10	670	###	0.68	17	0.3911	0.4115	1.89E+06	0.636	0.4350	35%	10%
Crushed rock		268.19	2.61	1.6	260	###	1.67	16	0.3938	1.0141	1.26E+05	1.115	0.4300	9%	8%
Crushed rock		268.19	1.61	1	100	###	1.66	10	0.4622	0.8950	1.62E+05	1.750	0.4650	49%	1%
Crushed rock		**268.19**	**1.28**	**0.5**	**50**	###	**2.10**	**8**	**0.4992**	**1.0501**	**9.35E+04**	**2.380**	**0.4470**	**56%**	**-12%**
Crushed rock		**268.19**	**0.59**	**0.8**	**20**	###	**1.13**	**4**	**0.6447**	**0.4012**	**1.19E+06**	**3.330**	**0.5000**	**88%**	**-29%**
Glass spheres		**268.19**	**0.95**	**3.23**	**81**	###	**0.71**	**6**	**0.5517**	**0.3183**	**3.01E+06**	**1.300**	**0.3550**	**76%**	**-55%**
Glass spheres		**268.19**	**0.87**	**2.93**	**68**	###	**0.71**	**5**	**0.5674**	**0.3092**	**3.17E+06**	**1.700**	**0.3610**	**82%**	**-57%**
Glass spheres		**268.19**	**0.75**	**2.79**	**53**	###	**0.68**	**5**	**0.5965**	**0.2742**	**4.23E+06**	**2.000**	**0.3670**	**86%**	**-63%**
Glass spheres		**268.19**	**0.64**	**1.98**	**35**	###	**0.74**	**4**	**0.6296**	**0.2755**	**3.83E+06**	**2.500**	**0.3810**	**89%**	**-65%**

Figure 14. *Our analysis of Shrinivas et al.*

As can be seen in Figure 14, a significant number of the reported samples fall outside our accept/reject criteria for external porosity (highlighted in bold). In addition, the author's reported values for d_p, the spherical particle diameter equivalent, and ε_0, the external porosity, are significantly different from our analysis values, and are indicated in the columns labeled Δd_p% and $\Delta\varepsilon_0$%, respectively. The discrepancies are significant and vary in both directions, i.e., some are larger and some are smaller than our values. We suggest that the experimental protocols used in this paper were not sufficiently accurate or precise to support the author's conclusions.

Example 7. Data of Salahi et al 2014

In our Figure 15 below, we present our analysis of the data set reported in a paper by Salahi et al., published in 2014 [54].

Sample ID	A	B	a	b	λ	d_c $\frac{1}{X^{1/\delta}Y^{1/\varepsilon}}$	δ $\frac{X^{1/\delta}}{100Y^{1/\varepsilon}}$	ε_0 $\frac{1}{\delta^{(1/3)}}$	d_p $d_c abs(1-\varepsilon_0)$	n_p $\frac{3D^2L(1-\varepsilon_0)}{2d_p^3}$	d reported	Δd %	ε_0 reported	$\Delta\varepsilon_0$ %
			sm^{-1}	$s^{-2}m^{-2}$		cm	none	none	cm					
Crushed														
a	268.19	1.45	1.7886	114.04	###	1.180	9.11	0.4788	0.615	1.35E+05	1.662	63%	0.4692	2%
b	268.19	2.29	1.0664	174.42	###	1.920	14.37	0.4113	1.130	2.45E+04	1.308	14%	0.4392	-7%
c	268.19	2.50	3.5081	361.70	###	1.106	15.71	0.3993	0.665	1.23E+05	0.869	24%	0.4284	-7%
d	268.19	2.90	4.5496	514.30	###	1.046	18.21	0.3801	0.649	1.36E+05	0.555	-17%	0.4225	-11%
e	268.19	2.95	15.6650	979.71	###	0.569	18.54	0.3779	0.354	8.42E+05	0.355	0%	0.4210	-11%
f	**268.19**	**4.34**	**45.5150**	**2978.80**	###	**0.405**	**27.26**	**0.3323**	**0.270**	**2.03E+06**	**0.177**	**-53%**	**0.4200**	**-26%**
Rounded	268.19													
a	268.19	1.49	3.161	158.58	###	0.901	9.39	0.4741	0.474	2.97E+05	1.778	73%	0.4071	14%
b	268.19	1.89	3.657	242.70	###	0.942	11.87	0.4383	0.529	2.28E+05	1.213	56%	0.3978	9%
c	268.19	2.55	4.924	440.70	###	0.943	16.00	0.3968	0.569	1.97E+05	1.035	45%	0.3864	3%
d	268.19	2.39	7.712	501.49	###	0.730	15.02	0.4053	0.434	4.37E+05	0.653	34%	0.3830	5%
e	268.19	2.69	15.678	854.85	###	0.543	16.92	0.3895	0.332	1.00E+06	0.417	20%	0.3790	3%
f	**268.19**	**4.98**	**42.782**	**3548.80**	###	**0.447**	**31.28**	**0.3174**	**0.305**	**1.44E+06**	**0.210**	**-45%**	**0.3750**	**-18%**

Figure 15. *Our analysis of Salahi et al.*

As can be seen in Figure 15, again two of the conduits fall outside our acceptable window with respect to external

porosity. In addition, it is also clear that the author's experimental protocol for determining the values of d_p and ε_0 were not adequate. Their reported values for both these variables vary significantly in both directions as compared to our N-S solution for both rounded and crushed rocks.

Example 8. Data of Zhongxia Li et al 2019

In our Figure 16 below, we present our analysis of the data set reported in a paper by Li et al. published in 2019 [55].

Sample ID	A	B	a	b	λ	d_c	δ	ε_0	d_p	n_p	d	Δd	ε_0	$\Delta\varepsilon_0$
						$\frac{1}{X^{(1/6)}y^{(1/2)}}$	$\frac{X^{1/6}}{100Y^{1/2}}$	$\frac{1}{\delta^{(1/3)}}$	$d_c abs(1-\varepsilon_0)$	$\frac{3D^2L(1-\varepsilon_0)}{2d_p^3}$	reported	%	reported	%
			sm^{-1}	$s^{-2}m^{-2}$		cm	none	none	cm					
a	268.19	1.82	85.74	1106.89	###	0.1907	11.41	0.4442	0.1060	1.05E+07	0.1310	19%	0.36	19%
	268.19	**0.61**	**76.98**	**203.30**	###	**0.1165**	**3.82**	**0.6396**	**0.0420**	**1.10E+08**	**0.1460**	**71%**	**0.36**	**44%**
	268.19	**0.88**	**53.88**	**294.13**	###	**0.1671**	**5.51**	**0.5663**	**0.0725**	**2.56E+07**	**0.1620**	**55%**	**0.36**	**36%**
b	**268.19**	**7.38**	**113.27**	**10424.45**	###	**0.3346**	**46.37**	**0.2783**	**0.2414**	**1.15E+06**	**0.1700**	**-42%**	**0.36**	**-29%**
	268.19	**3.96**	**97.42**	**3803.17**	###	**0.2643**	**24.90**	**0.3425**	**0.1738**	**2.82E+06**	**0.2120**	**18%**	**0.36**	**-5%**
	268.19	1.80	67.84	970.01	###	0.2134	11.30	0.4457	0.1183	7.54E+06	0.2540	53%	0.36	19%
c	268.19	1.85	17.18	510.19	###	0.4303	11.63	0.4413	0.2404	9.05E+05	0.2250	-7%	0.36	18%
	268.19	2.30	13.59	628.74	###	0.5395	14.46	0.4104	0.3181	4.12E+05	0.2510	-27%	0.36	12%
	268.19	1.76	12.23	398.62	###	0.4971	11.05	0.4489	0.2739	6.03E+05	0.2770	1%	0.36	20%
d	268.19	1.91	28.17	683.36	###	0.3411	11.99	0.4369	0.1921	1.79E+06	0.1980	3%	0.36	18%
	268.19	2.10	24.02	728.96	###	0.3876	13.20	0.4231	0.2236	1.16E+06	0.2320	4%	0.36	15%
	268.19	2.53	16.85	808.05	###	0.5081	15.91	0.3976	0.3061	4.73E+05	0.2660	-15%	0.36	9%
a	268.19	1.80	78.21	1043.18	###	0.1988	11.31	0.4455	0.1102	9.31E+06	0.1075	-3%	0.36	19%
	268.19	2.53	59.71	1520.56	###	0.2699	15.91	0.3976	0.1626	3.15E+06	0.1075	-51%	0.36	9%
	268.19	3.48	53.68	2322.68	###	0.3337	21.86	0.3576	0.2143	1.47E+06	0.1075	-99%	0.36	-1%
b	268.19	2.04	55.50	1057.10	###	0.2510	12.79	0.4276	0.1437	4.34E+06	0.1475	3%	0.36	16%
	268.19	1.91	45.47	866.62	###	0.2683	11.97	0.4371	0.1510	3.68E+06	0.1475	-2%	0.36	18%
	268.19	2.35	31.13	982.20	###	0.3601	14.77	0.4076	0.2134	1.37E+06	0.1475	-45%	0.36	12%
c	268.19	2.01	37.54	853.48	###	0.3033	12.63	0.4293	0.1731	2.48E+06	0.1850	6%	0.36	16%
	268.19	2.32	25.05	866.72	###	0.3993	14.61	0.4091	0.2359	1.01E+06	0.1850	-28%	0.36	12%
	268.19	2.34	19.77	776.06	###	0.4506	14.68	0.4084	0.2666	7.02E+05	0.1850	-44%	0.36	12%

Figure 16. *Our analysis of the data of Li et al.*

As can be seen in Figure 16, just 4 of the samples fall outside our acceptable window for external porosity. In addition, it is also clear, again that the author's experimental protocol for determining the values of d_p and ε_0 were not adequate. Their reported values for both these variables vary significantly in both directions as compared to our N-S solution for these particles of quartz sands. Furthermore, since the authors state that all packed conduits had the identical same value for external porosity, i.e., 0.36, we are inclined to reject the entire premise of this paper as an example of empirical data, but include it as part of our selected examples to alert the reader to the fact that the literature is filled with these type of "measurement" examples.

Example 9. Data of Neue et al 2005

In our Figure 17 below, we include our evaluation of a paper by Neue et al., published in 2005 [56]. This paper represents a category of packed conduits of commercial value for the high efficiency analysis of small molecules of interest in the pharmaceutical industry. The chromatographic "columns" as they are referred to in the industry, are used in the application of HPLC, i.e., high pressure liquid chromatography.

Sample ID	R_{em}	A	B	a	b	λ	d_c	δ	ε_0	d_p	n_p	d	Δd	ε_0	$\Delta\varepsilon_0$
							$\frac{1}{X^{(1/6)}y^{(1/2)}}$	$\frac{X^{1/6}}{Y^{1/2}}$	$\frac{1}{\delta^{(1/3)}}$	$d_c abs(1-\varepsilon_0)$	$\frac{3D^2L(1-\varepsilon_0)}{2d_p^3}$	reported	%	reported	%
	none			sm^{-1}	s^2m^{-2}		cm	none	none	cm		cm		none	
2005															
1	0.00848	268.19	2.36	5,097	0.0127	1.0000	0.000280	14.83	0.4070	0.000166	4.28E+10	0.000170	2%	0.3640	11%
2	0.00676	268.19	2.78	796	0.0064	1.0000	0.000769	17.47	0.3854	0.000473	1.92E+09	0.000480	1%	0.3570	7%
3	0.00490	268.19	2.43	5,305	0.0136	1.0000	0.000279	15.29	0.4029	0.000166	4.29E+10	0.000170	1%	0.3630	7%
4	0.01604	268.19	2.47	682	0.0050	1.0000	0.000783	15.50	0.4011	0.000469	1.92E+09	0.000480	2%	0.3570	10%

Figure 17. *HPLC Columns.*

As can be seen in Figure 17, these packed conduits contain small spherical particles operated at relatively high pressure drops. Note that there is relatively good agreement in our analysis between the values reported by the paper authors for particle diameter. However, the values for external porosity reported by the authors are typically 10-15% too low,

representing as they do: (a) an embedded assumption in the author's paper, that the value of the constant A in the Kozeny-Carman equation is always 180, and (b) the fact that only a solitary measurement of permeability was made for each sample at extremely low values of the modified Reynolds number, thus, totally ignoring kinetic considerations.

Example 10. Data of Cabooter et al 2008

In our Figure 18 below, we include our evaluation of a paper by Cabooter et al. published in (2008) [57]. This paper is also an example of HPLC columns but represents the most modern version thereof, typically referred to in the industry as UHPLC, i.e. ultra high pressure liquid chromatography. Additionally, this paper allows us to underscore a fundamental issue which appears time and time again, particularly, in the chromatographic literature. That issue is the fact that the Laws of Continuity are generally ignored with respect to the utilization of free space within a packed conduit. This issue raises its' head in this example, since the authors report the use of several different particle diameter choices but report just one set of external porosities and one set of pressure drop measurements and, moreover, totally ignore the number of particles, or an equivalent reconciliation, for each of the respective sets of particle diameter values reported. We have chosen herein just one of the reported sets of values for particle diameter, i.e., that provided by the manufacturer of the particles.

Sample ID	R_{em}	A	B	a	b	λ	d_c $\frac{1}{X^{(1/6)}Y^{(1/2)}}$	δ $\frac{X^{1/6}}{Y^{1/2}}$	ε_0 $\frac{1}{\delta^{(1/3)}}$	d_p $d_c abs(1-\varepsilon_0)$	n_p $\frac{3D^2L(1-\varepsilon_0)}{2d_p^3}$	d reported	Δd %	ε_0 reported	$\Delta\varepsilon_0$ %
	none			sm^{-1}	s^2m^{-2}		cm	none	none	cm		cm		none	
2005															
Hypersil Gold C18	0.00013	268.19	1.87	3,492	0.0068	1.0000	0.000329	12	0.4398	0.000185	2.95E+10	0.000190	3%	0.3880	12%
Hypersil Gold C18	0.00013	268.19	2.03	3,984	0.0082	1.0000	0.000321	13	0.4278	0.000184	3.04E+10	0.000190	3%	0.3690	14%
Zorbax C18	0.00012	268.19	2.13	4,642	0.0095	1.0000	0.000305	13	0.4213	0.000176	3.49E+10	0.000180	2%	0.3840	9%
Zorbax C18	0.00003	268.19	2.10	4,533	0.0092	1.0000	0.000306	13	0.4234	0.000176	1.66E+11	0.000180	2%	0.3880	8%
Acquity BEH C18	0.00012	268.19	1.90	4,601	0.0080	1.0000	0.000289	12	0.4375	0.000163	4.32E+10	0.000170	4%	0.3580	18%
Acquity BEH C18	0.00012	268.19	2.02	4,929	0.0091	1.0000	0.000288	13	0.4286	0.000165	4.23E+10	0.000170	3%	0.3480	19%

Figure 18. *UHPLC columns.*

As shown in Figure 18, the particle diameters are even smaller in these type columns and are typically in the range of 2-3 microns. Again, note that there is relatively good agreement in our analysis between the values reported by the paper authors for particle diameter. However, the values for external porosity reported by the authors are, once again, typically 10-20% too low, due to: (a) an embedded assumption in the author's paper, that the value of the constant A in the Kozeny-Carman equation is not constant, but varies as a function of particle size distribution and, (b) the authors totally ignored the porosity of these particles, ε_p, (an independent variable whose value is available from the particle manufacturer) and, accordingly, made no attempt to reconcile the packed conduit internal porosity, ε_i, thus, violating the Laws of Continuity for packed conduits and, (c) the fact that only a solitary measurement of permeability was made for each sample, at extremely low values of the modified Reynolds number, thus, totally ignoring kinetic considerations.

5. Conclusions

In this paper, we have demonstrated a unique solution to the Navier-Stokes equation for closed conduits, both packed and empty. In so doing, we have used both the underlying theory and equation expressed in Quinn's Law, to arrive at a boundary condition which identifies the value of λ at one specific flow rate for any given fluid flow experiment under study. This is both a necessary and sufficient condition to identify, simultaneously, the unique combination of the values of d_p and ε_0 in any closed conduit under study, and which, in combination with the measured Forchheimer coefficients of a, and b, can correlate precisely any measured data at any point across the entire spectrum of the modified Reynolds number, which includes the regions typically referred to in conventional wisdom as, laminar, transitional and fully turbulent. We have also evaluated several examples of empirical data including both packed and empty conduits, from our own laboratory as well as those taken from published third party laboratories. Our conclusions based upon our application of this unique solution to the N-S equation can be catalogued as follows:

1. The value of the coefficient A in the re-invented Ergun model, i.e., the Q-modified Ergun equation, has the constant value of $256\pi/3$ which is 268.19 approx.
2. The value of the coefficient B in the re-invented Ergun model, i.e., the Q-modified Ergun equation, is a variable function of the external porosity of the conduit as well as the wall normalization coefficient λ. Thus, the typical value of B falls in a range from 1.5 to 3.5 for well-packed conduits packed with rigid particles having a solid skeleton and a large ratio for D/d_p.
3. There is but one unique combination of values for d_p, ε_0 and n_p which will correlate permeability measurements over the entire range of the fluid flow profile, from creeping flow to fully turbulent flow. This is a result of the Laws of Nature which dictate that for any given conduit under study, every combination of the packed conduit values of the variables d_p and n_p represents a unique hypothetical Q channel and, consequently, a

unique pressure gradient/fluid flow rate profile over the entire fluid flow regime. This relationship between pressure gradient and fluid flow rate is quadratic over the entire range of flow rates in any given packed conduit under study.

4. The Laws of Continuity dictate that for any given conduit dimensions, i.e. diameter D and length L, packed with rigid particles of spherical particle diameter equivalent, d_p, the value of ε_0 is not an independent variable but is defined by the combination of the values of d_p and n_p, i.e. the number of particles present in the packed conduit.
5. In order to accurately define the Forchheimer coefficients a, and b, empirical measurements must be taken in the nonlinear portion of the fluid flow regime, i.e. where kinetic contributions are significant. This is a result of the fact that kinetic contributions are much more sensitive to the value of the external porosity parameter, ε_0, than are viscous contributions.
6. In most engineering examples studied in the literature, the experimental protocols typically used to measure the values of d_p and ε_0 are not sufficiently accurate or precise to validate the value of these variables using pressure drop measurements. Measurement discrepancies occur in both directions, i.e., both larger and smaller than the actual values. Thus, the values reported in the literature have values for external porosity which are both too high and too low.
7. In most chromatographic examples studied in the literature, on the other hand, the experimental protocols typically used to identify the values of d_p and ε_0 are fundamentally flawed for several reasons. Firstly, they are based upon a back calculation of permeability which is derived based upon the erroneous assumption that the value of the coefficient in the Kozeny-Carman fluid flow model is either constant at 180 approx., or varies as a function of the particle size distribution, secondly, the values for d_p and ε_0 are both independently measured, without any reconciliation with the value of n_p, thus violating the Conservation Laws as applied to the total amount of free space contained within the empty conduit under study, thirdly, pressure drop measurements are typically taken in the linear portion of the fluid flow regime (laminar) thus totally ignoring kinetic contributions, fourthly, particle porosity is sometimes substituted for conduit internal porosity and, finally, mobile phase velocity is sometimes substituted for superficial fluid velocity. These errors typically result in reported values of permeability, which do not facilitate accurate identification of underlying fluid embodiment variables based upon measured pressure drops, most notably external porosity, which is invariable 10-15% too low.

Declaration of Interest

The author declares no conflict of interest.

Appendix

Ref: Quinn's Law of Fluid Dynamics Pressure-driven Fluid Flow Through Closed Conduits. *Fluid Mechanics*. Vol. 5, No. 2, 2019, pp. 39-71. doi: 10.11648/j.fm.20190502.12.

Table 1. *Glossary of Terms.*

#	Symbol	Unit cgs	Ref.	Formula	Description
				Particle	Independent variable
1	d_{pm}	cm	Sec 2.2.1	N/A	Particle nominal diameter
2	Ω_p	none	Sec 2.2.1	N/A	Particle sphericity
3	S_{pv}	cm^3g^{-1}	Sec 2.2.1	N/A	Particle specific pore volume
4	ρ_{sk}	gcm^{-3}	Sec 2.2.1	N/A	Particle skeletal density
5	m_{dp}	g	Sec 2.2.1	N/A	Mass of the particle
					Dependent variable
6	d_p	cm	Eq (1)	$\Omega_p d_{pm}$	Spherical particle diameter equivalent
7	SA_p	cm^2	Eq (2)	πd_p^2	Surface area of spherical particle equivalent
8	CSA_p	cm^2	Eq (3)	$\pi d_p^2/4$	Cross-sectional area of spherical particle equivalent
9	V_{dp}	cm^3	Eq (4)	$\pi d_p^3/6$	Volume of spherical particle equivalent
10	ρ_{part}	g	Eq (5)	m_{dp}/V_{dp}	Particle apparent density
11	ε_p	none	Eq (6)	$S_{pv}\rho_{part}$	Particle porosity
				Conduit	Independent variable
12	D	cm	Sec 2.2.2	N/A	Conduit diameter
13	L	cm	Sec 2.2.2	N/A	Conduit length
14	k	cm	Sec 2.2.2	N/A	Conduit wall roughness dimension
15	n_p	none	Sec 2.2.2	N/A	Number of particle equivalents in conduit under study
					Dependent variable
16	V_{ec}	cm^3	Eq (7)	$\pi D^2L/4$	Empty conduit volume expressed in terms of conduit diameter and length
17	V_{part}	cm^3	Eq (8)	n_pV_{dp}	Conduit volume occupied by all the particles
18	n_{pq}	none	Eq (9)	$3D^2L/(2d_p^3)$	Dimensionless empty conduit volume (number of spherical particle equivalents)

#	Symbol	Unit cgs	Ref.	Formula	Description
19	γ	none	Eq (10)	$n_{pq}D/L$	Conduit architectural coefficient
				Q porosity Functions	Independent variable
20	V_e	cm^3	Sec 2.2.2	N/A	Conduit volume *external* to the particle fraction
21	V_i	cm^3	Sec 2.2.2	N/A	Conduit volume *internal* to the particle fraction
22	V_{sk}	cm^3	Sec 2.2.2	N/A	Conduit volume occupied by the cumulative skeletons of all the particles
23	V_t	cm^3	Sec 2.2.2	N/A	Conduit volume excluding the volume occupied by the particle skeletons
					Dependent variable
24	$(1-\varepsilon_0)$	none	Eq (11)	n_p/n_{pq}	Conduit particle volume fraction
25	ε_0	none	Eq (12)	$(1-n_p/n_{pq})$	Conduit external porosity; volume fraction external to particles
26	ε_i	none	Eq (13)	$\varepsilon_p(1-\varepsilon_0)$	Conduit internal porosity; volume fraction internal to particles (porous)
27	ε_t	none	Eq (14)	$1-(1-\varepsilon_p)n_p/n_{pq}$	Conduit total porosity; sum of external and internal volume fraction (porous)
28	ε_{sk}	none	Eq (15)	$n_p(1-\varepsilon_p)/n_{pq}$	Conduit skeletal porosity; volume fraction occupied by skeleton of particle fraction
29	$n_p\pi d_p^3/6$	none	Eq (16)	$V_{ec}abs(1-\varepsilon_0)$	Reconciliation between solids and porosity in packed conduit
				Governing Principle	Continuity Laws
32	Unity	none	Eq (17)	$\varepsilon_0 + \varepsilon_i + \varepsilon_{sk}$	Conservation Law (porous particles)
33	Unity	none	Eq (18)	$\varepsilon_t + \varepsilon_{sk}$	Conservation Law
34	ρ_{pack}	gcm^{-1}	Eq (19)	M_p/V_{ec}	Conduit packing density
35	ε_0	none	Eq (20)	$1-\rho_{pack}(S_{pv}-1/\rho_{sk})$	Conduit external porosity (mass of particles based)
36	ε_0	none	Eq (21)	$1-(2n_pd_p^3/(3D^2L))$	Conduit external porosity (number of particles based)
37	ε_p	none	Eq (22)	$(\varepsilon_t-\varepsilon_o)/(1-\varepsilon_0)$	Particle porosity (measurements made *inside* packed conduit)
38	$S_{pv}\rho_{part}$	none	Eq (23)	$(\varepsilon_t-\varepsilon_o)/(1-\varepsilon_0)$	Particle porosity (measurements made *outside* packed conduit) i.e. *independent*
39				Hypothetical Q Channel	Dimensional parameters (scale factor)
40	d_c	cm	Eq (24)	$d_p/(abs(1-\varepsilon_0))$	HQC diameter under study
41	v_c	cm^3	Eq (25)	$\pi n_{pq}d_p^3\varepsilon_t/6$	HQC volume under study
42	a_c	cm^2	Eq (26)	$\pi n_{pq}^2d_p^2/(4n_p^2)$	HQC cross sectional area
43	l_c	cm	Eq (27)	$2n_p^2d_p\varepsilon_t/(3n_{pq})$	HQC length under study
					Uniform Circular motion
44	ΔP	$gcm^{-1}sec^{-2}$	Eq (28)	P_1-P_0	Conduit Differential pressure
45	ω	$radsec^{-1}$	Eq (29)	$d\Phi/dt$	Angular velocity
46	Φ	radians	Eq (30)	$(\omega t + \alpha)$	Phase of the motion
47	x	cm	Eq (31)	$Acos(\omega t+\alpha)$	x coordinate displacement
				QFFM	Dimensionless manifestation
48	P_Q	none	Eq (32)	$(k_1 + \lambda Q_N/\phi_h)$	Viscous normalized friction factor
49	P_K	none	Eq (33)	P_Q/Q_N	Kinetic normalized friction factor
50	Θ	none	Eq (34)	Q_N/P_Q	Dimensionless permeability
51	Θ	none	Eq (35)	$1/(k_1/Q_N+\lambda/\phi_h)$	Dimensionless permeability
				QFFM	Reference parameters
52	π	none	N/A	22/7	Universal constant
53	ϕ_h	none	Eq (36)	$2\pi r_h=8\pi$	Drag normalized hydraulic channel circumference
54	k_2		Eq (37)	$1/\phi_h=1/(8\pi)$	Fluid kinetic control element normalization coefficient
55	r_h	none	Eq (38)	$SA_p/CSA_p=4$	Normalization coefficient of fluid drag
56	k_1	none	Eq (39)	$4/3\pi r_h^2=67$	Fluid viscous control element normalization coefficient
				Fluid Dynamics	Parameters
57	P_Q	none	Eq (40)	$64\pi/3+\lambda Q_N/8\pi$	Viscous normalized friction factor
58	δ	none	Eq (41)	$1/\varepsilon_0^3$	Conduit porosity normalization coefficient
59	τ	none	Eq (42)	$\delta\gamma$	Conduit tortuosity normalization coefficient
60	Q_N	none	Eq (43)	δR_{em}	Fluid current
61	λ	none	Eq (44)	$(1+W_N)$	Fluid current wall normalization coefficient
62	P_Q	none	Eq (45)	$64\pi/3+\delta\lambda R_{em}/(2\pi r_h)$	Viscous normalized friction factor
63	P_Q	none	Eq (46)	$64\pi/3+\delta(1+W_N)R_{em}/(2\pi r_h)$	Viscous normalized friction factor
64	W_N	none	Eq (47)	$W_1 + W_{2R}$	Net wall effect
65	ω	none	Eq (48)	$1/\phi_h$	Dimensionless fluid resistance
66	β	none	Eq (49)	$k_1/(k_2Q_N+k_1)$	Viscous boundary layer (λ=1)
67	W_1	none	Eq (50)	$\beta_0^{(1/3)}/\tau$	Primary wall effect
68	k_{dc}	none	Eq (51)	k/d_c	Relative wall roughness coefficient
69	W_2	none	Eq (52)	$30k_{dc}^{(1/3)}$	Secondary wall effect
70	W_{2R}	none	Eq (53)	$W_2-W_1^{(1.2)}$	Residual secondary wall effect ($W_{2R} \geq 0$)
71	R_{em}	none	Eq (54)	$4qd_c\rho_f/(\pi\eta D^2)$	Modified Reynolds number
72	n_k	$gcm^{-2}sec^{-2}$	Eq (55)	$\delta\mu_s^2\rho_f/d_c$	the *kinetic* hydraulic force exerted *per unit element of fluid control volume*
73	μ_s	$cmsec^{-1}$	Eq (56)	$4q/(\pi D^2)$	Average fluid superficial linear velocity (fluid flux).
74	n_v	$gcm^{-2}sec^{-2}$	Eq (57)	$\delta\mu_s\eta/d_c^2$	the *viscous* hydraulic force exerted *per unit element of fluid control volume*
75	BLT	cm	Eq (58)	$\beta d_c/(2\tau)$	Boundary layer thickness
76	P_Q	none	Eq (59)	$4\pi r_h^2/3 + \delta\lambda n_k/(2\pi r_h n_v)$	Viscous friction factor
77	$\Delta P/(r_h n_v L)$	none	Eq (60)	P_Q	Drag normalized viscous friction factor
78	$\Delta P/(r_h n_v L)$	none	Eq (61)	$4\pi r_h^2/3 + \delta\lambda n_k/(2\pi r_h n_v)$	Drag normalized viscous friction factor

#	Symbol	Unit cgs	Ref.	Formula	Description
79	$\Delta P/(r_h L)$	$gcm^{-2}sec^{-2}$	Eq (62)	$4\pi r_h^2 n_v/3 + \delta\lambda n_k/(2\pi r_h)$	Drag normalized pressure gradient
80	$\Delta P/L$	$gcm^{-2}sec^{-2}$	Eq (63)	$4\pi r_h^3 n_v/3 + \delta\lambda n_k/2\pi$	Total pressure gradient
81	$\Delta P/L$	$gcm^{-2}sec^{-2}$	Eq (64)	$4\pi r_h^3\delta\mu_s\eta/(3d_c^2) + \delta\ \lambda\mu_s^2\rho_f/dc$	QFFM practitioner's empirical equation
82	$\Delta P/L$	$gcm^{-2}sec^{-2}$	Eq (65)	$4\pi r_h^3 n_v/3$	Viscous pressure gradient
83	C_Q	none	Eq (66)	λQ_N	Wall normalized instantaneous fluid current
84	β	none	Eq (67)	$k_1/(k_2 C_Q + k_1)$	Instantaneous boundary layer
85	P_Q	none	Eq (68)	$64\pi/3 + C_Q/(8\pi)$	Quinn's Law
86	$\Delta P/L$	$gcm^{-2}sec^{-2}$	Eq (69)	$1024\delta q\eta/(3D^2d_c^2) + 8\delta^2\lambda q^2\rho_f/(\pi^3 D^4 d_c)$	QFFM expanded equation
87	$\Delta P/L$	$gcm^{-2}sec^{-2}$	Eq (70)	$128q\eta/(3D^4) + \lambda q^2\rho_f/(248D^5)$	QFFM balanced equation for empty conduit
				QFFM	Dimensional manifestation
88	q	$cm^3sec\text{-}1$	Sec 2.3.3	dv/dt	Fluid volumetric flow rate
89	η	$gcm^{-1}sec^{-1}$	Sec 2.3.3	N/A	Fluid absolute viscosity
90	ρ_f	gcm^{-3}	Sec 2.3.3	N/A	Fluid density
91	ν	cm^2sec^{-1}		η/ρ_f	Fluid kinematic viscosity
92	λ_{bc}	none		$\pi^3 D^4 d_c(\Delta P\text{-}bq)/(8\delta^2\rho_f L q^2)$	Back-calculated wall normalization coefficient
93	QFFM	none	Eq (71)	$aq^2+bq+c=0$	Quadratic manifestation
94	c	$gcm^{-1}sec^{-2}$	Eq (72)	$-\Delta P$	constant
95	ΔP	$gcm^{-1}sec^{-2}$	Eq (73)	$aq^2 + bq$	Calculated differential pressure drop
96	q_{bc}	m^3sec^{-1}	Eq (74)	$-b\pm\sqrt{(b^2-4ac)}/(2a)$	Back-calculated flow rate from measured pressure differential
97	a	gcm^{-7}	Eq (75)	$8\delta^2\lambda\rho_f L/(\pi^3 D^4 d_c)$	Quadratic term coefficient (flow rate based)
98	b	$gcm^{-4}sec^{-1}$	Eq (76)	$1024\delta\eta L/(3D^2d_c^2)$	Linear term coefficient (flow rate based)
99	$\Delta P/L$	$gcm^{-2}sec^{-2}$	Eq (77)	$1024(1\text{-}\varepsilon_0)^2 q\eta/(3D^2d_c^2) + 8(1\text{-}\varepsilon_0)\ \lambda q^2\rho_f/(\pi^3 D^4\varepsilon_0^6 d_c)$	Total pressure gradient
100	$\Delta P/L$	$gcm^{-2}sec^{-2}$	Eq (78)	$256\pi(1\text{-}\varepsilon_0)^2\mu_s\eta/3\varepsilon_0^3 d_p^2 + (1\text{-}\varepsilon_0)\lambda\rho_f\ \mu_s^2/(2\pi\varepsilon_0^6 d_p)$	Q modified Ergun equation
101	$\Delta P/L$	$gcm^{-2}sec^{-2}$	Eq (79)	$A(1\text{-}\varepsilon_0)^2\mu_s\eta/(\varepsilon_0^3 d_p^2) + B(1\text{-}\varepsilon_0)\rho_f\ \mu_s^2/(\varepsilon_0^3 d_p)$	Q modified Ergun equation
102	A	none	Sec. 2.34	$256\pi/3$	Q modified Ergun (viscous) constant
103	B	none	Sec. 2.34	$\lambda/(2\pi e_0^3)$	Q modified Ergun (kinetic) constant
104	τ_w	$gcm^{-1}sec^{-2}$	Eq (82)	$\Delta PD/(4L)$	Wall shear stress
				Harmonic Oscillator	Parameters
					Damping Coefficients
105	v	$cmsec^{-1}$	Eq (80)	$v_x + v_y + v_z$	Instantaneous fluid velocity
106	t_0	sec	Eq (81)	$(\pi D^2 L\varepsilon_t)/4q$	Time to displace one (packed) conduit volume
107	μ_f	$cmsec^{-1}$	Eq (83)	$(\tau_w/\rho_f)^{(1/2)}$	Fluid frictional velocity
					SHM dimensional parameter equivalents
108	t	sec	Sec 3	Q_N	Elapsed time
109	α	radians	Sec 3	$k_1(2\pi/360)$	Epoch of the motion
110	ω_0	$radsec^{-1}$	Sec 3	k_2	Reference angular velocity (when there is no net wall effect; $W_N=0$; $\lambda=1$)
111	ω	$radsec^{-1}$	Sec 3	λ/ϕ_h	Instantaneous angular velocity
112	Φ	radians	Sec 3	P_Q	Phase of the motion
113	T	sec	Eq (84)	$2\pi/\omega$	Period of the motion
114		$radsec^{-1}$	Eq (85)	1/T	Frequency of the motion
115	M_0	cm	Eq (86)	$d_c/2$	Maximum amplitude displacement (scale factor)
116	M	cm	Eq (87)	$M_0 exp^{(-\omega to)}$	Instantaneous amplitude displacement
					Dimensional x-coordinate
117	x	cm	Eq (88)	$M cos P_Q$	Instantaneous displacement in x direction
118	V_x	$cmsec^{-1}$	Eq (89)	$-M\lambda/\ _h sin P_Q$	Instantaneous velocity in x direction
119	f_x	$cmsec^{-2}$	Eq (90)	$-M(\lambda/\ _h)^2 cos P_Q$	Instantaneous acceleration in x direction
					Dimensional y-coordinate
120	y	cm	Eq (91)	$M sin P_Q$	Instantaneous displacement in y direction
121	V_y	$cmsec^{-1}$	Eq (92)	$M(\lambda/\phi_h) cos P_Q$	Instantaneous velocity in y direction
122	f_y	$cmsec^{-2}$	Eq (93)	$-M(\lambda/\phi_h)^2 sin P_Q$	Instantaneous acceleration in y direction
					Dimensional z-coordinate
123	z	cm	Eq (94)	$M cos(\pi/4\text{-}P_Q)$	Instantaneous displacement in y direction
124	V_z	$cmsec^{-1}$	Eq (95)	$-M(\lambda/\phi_h) sin(\pi/4\text{-}P_Q)$	Instantaneous velocity in y direction
125	f_z	$cmsec^{-2}$	Eq (96)	$-M(\lambda/\phi_h)^2 cos(\pi/4\text{-}P_Q)$	Instantaneous acceleration in y direction
					Dimensionless x-coordinate
126	x*	none	Eq (97)	$(M_0\text{-}x)/(2M_0)$	Unit cell displacement in x direction
127	V_x*	none	Eq (98)	V_x/μ_f	Unit cell velocity in x direction
					Dimensionless y-coordinate
128	y*	none	Eq (99)	$(M_0\text{-}y)/(2M_0)$	Unit cell displacement in y direction
129	V_y*	none	Eq (100)	V_y/μ_f	Unit cell velocity in y direction
					Dimensionless z-coordinate

#	Symbol	Unit cgs	Ref.	Formula	Description
130	z*	none	Eq (101)	$(M_0\text{-}z)/(2M_0)$	Unit cell displacement in z direction
131	V_z*	none	Eq (102)	V_z/μ_f	Unit cell velocity in y direction

References

[1] Poiseuille, J. L. (1841). "Recherches expérimentales sur le mouvement des liquides dans les tubes de très-petits diamètres." Comptes Rendus, Académie des Sciences, Paris 12, 112 (in French).

[2] H. Darcy, *Les Fontaines Publiques de la Ville de Dijon*, Victor Dalmont, Paris, France, 1856.

[3] J. L. M. Poiseuille, Memoires des Savants Etrangers, Vol. IX pp. 435-544, (1846);. Brillouin, Marcel (1930). "Jean Leonard Marie Poiseuille". *Journal of Rheology*. 1: 345. doi: 10.1122/1.2116329.

[4] H. M. Quinn, "Reconciliation of packed column permeability data, column permeability as a function of particle porosity," *Journal of Materials*, vol. 2014, Article ID 636507, 22 pages, 2014.

[5] J. M. Coulson; University of London, Ph. D. thesis, "The Streamline Flow of Liquids through beds comprised of Spherical particles" 1935.

[6] A. O. Oman and K. M. Watson, "Pressure drops in granular beds," *National Petroleum News*, vol. 36, pp. R795–R802, 1944.

[7] M. Leva and M. Grummer, "Pressure drop through packed tubes, part I, a general correlation," vol. 43, pp. 549–554, 1947.

[8] F. A. L. Dullien, *Porous Media, Fluid Transport and Pore Structure*, Acedemic Press, 2nd edition, 1979.

[9] S. W. Churchill, *Viscous Flows: The Practical Use of Theory*, Butterworks, 1988.

[10] S. P. Burke and W. B. Plummer, "Gas flow through packed columns," *Industrial and Engineering Chemistry*, vol. 20, pp. 1196–1200, 1923.

[11] J. C. Giddings, Dynamics of Chromatography, Part I, Principles and Theory, Marcel Dekker, Inc. New York, 1965.

[12] T. Farkas, G. Zhong, G. Guiochon, Journal of Chromatography A, 849, (1999) 35-43.

[13] M. Rhodes, Introduction to Particle technology, John Wiley & Sons, Inc., p. 83 (1998).

[14] G. O. Brown., 1999-2006, Henry Darcy and His Law, www.biosystems.okstate.edu/Darcy.

[15] I. Halász, R. Endele, and J. Asshauer, "Ultimate limits in high-pressure liquid chromatography," *Journal of Chromatography A*, vol. 112, no. C, pp. 37–60, 1975.

[16] F. E. Blake, "The resistance of packing to fluid flow," *Transaction of American Institute of Chemical Engineers*, vol. 14, pp. 415–421, 1922.

[17] J. Kozeny, "Uber kapillare Leitung des wassers in Böden," *Sitzungsberichte der Kaiserlichen Akademie der Wissenschaften*, vol. 136, pp. 271–306, 1927.

[18] Carman, P. C., "Fluid flow through granular beds," Transactions of the Institution of Chemical Engineers, vol. 15, pp. 155–166, 1937.

[19] Bird, R. B., Stewart, W. E., Lightfoot, E. N. Transport Phenomena, John Wiley & Sons, Inc., p. 190.

[20] H. M. Quinn, Reconciliation of Packed Column Permeability Data-Part 1. The Teaching Of Giddings Revisited, Special Topics & Reviews in Porous Media-An International Journal 1 (1), (2010) 79-86.

[21] I. Halasz, M. Naefe, Analytical Chemistry, 44 (1972) 76

[22] G. Guiochon, Chromatographic Review, 8 (1966).

[23] A. E. Scheidegger, *The Physics of Flow Through Porous Media*, MacMillan Company, New York, NY, USA, 1957.

[24] J. Kozeny, "Ueber kapillare Leitung des Wassers im Boden." Sitzungsber Akad. Wiss., Wien, 136 (2a): 271-306, 1927.

[25] J. C. Giddings, Unified Separation Science, John Wiley & Sons (1991).

[26] Halasz, R. Endele, K. Unger, Journal of Chromatography, 99 (1974) 377-393.

[27] U. Neue, HPLC Columns-Theory, Technology and Practice, Wiley-VCH (1997).

[28] P. C. Carman, Trans. Instn. Chem. Engrs. Vol. 15, (1937) 155-166.

[29] J. M. Godinho, A. E. Reising, U. Tallarek, J. W. Jorgenson; Implementation of high slurry concentration and sonication to pack high-efficiency, meter-long capillary ultrahigh pressure liquid chromatography columns: Journal of Chromatography A, 1462 (2016) 165-169.

[30] L. R. Snyder, J. J. Kirkland, Introduction to Modern Liquid Chromatography, 2nd Edition, John Wiley & Sons, Inc. p. 37 (1979).

[31] G. Guiochon, S. G. Shirazi, A. M. Katti, Fundamentals of Preparative and Nonlinear Chromatography, Academic Press, Boston, Ma, (1994).

[32] S. Ergun and A. A. Orning, "Fluid flow through randomly packed columns and fluidized beds," *Industrial & Engineering Chemistry*, vol. 4, no. 6, pp. 1179–1184, 1949.

[33] Ergun, Chem. Eng. Progr. 48 (1952) 89-94.

[34] I. F. Macdonald, M. S. El-Sayed, K. Mow, and F. A. L. Dullien *Industrial & Engineering Chemistry Fundamentals* 1979 *18* (3), 199-208 DOI: 10.1021/i160071a001.

[35] J. Happel and H. Brenner, *Low Reynolds Number Hydrodynamics*, Prentice-Hall, 1965.

[36] Reynolds O. 1883. An experimental investigation of the circumstances which determine whether the motion of water in parallel channels shall be direct or sinuous and of the law of resistance in parallel channels. Philos. Trans. R. Soc. 174: 935–82.

[37] J. Nikuradze, NASA TT F-10, 359, Laws of Turbulent Flow in Smooth Pipes. Translated from "Gesetzmassigkeiten der turbulenten Stromung in glatten Rohren" VDI (Verein Deutsher Ingenieure)-Forschungsheft 356.

[38] J. Nikuradze, NACA TM 1292, Laws of Flow in Rough Pipes, July/August 1933. Translation of "Stromungsgesetze in rauhen Rohren." VDI-Forschungsheft 361. Beilage zu "Forschung auf dem Gebiete des Ingenieurwesens" Ausgabe B Band 4, July/August 1933.

[39] L. Prandtl, in Verhandlungen des dritten internationalen Mathematiker-Kongresses in Heidelberg 1904, A. Krazer, ed., Teubner, Leipzig, Germany (1905), p. 484. English trans. in Early Developments of Modern Aerodynamics, J. A. K. Ackroyd, B. P. Axcell, A. I. Ruban, eds., Butterworth-Heinemann, Oxford, UK (2001), p. 77.

[40] Moody, L. F. (1944). "Friction factors for pipe flow." Trans. ASME, 66: 671-678.

[41] Studies and Research on Friction, Friction Factor and Affecting Factors: A Review Sunil J. Kulkarni *, Ajaygiri K. Goswami; Chemical Engineering Department,, Datta Meghe College of Engineering, Airoli, Navi Mumbai, Maharashtra, India.

[42] Technical Note: Friction Factor Diagrams for Pipe Flow; Jim McGovern Department of Mechanical Engineering and Dublin Energy Lab Dublin Institute of Technology, Bolton Street Dublin 1, Ireland.

[43] B. J. Mckeon, C. J. Swanson, M. V. Zagarola, R. J. Donnelly and A. J. Smits. Friction factors for smooth pipe flow; J. Fluid Mech. (2004), vol. 511, pp. 41-44. Cambridge University Press; DO1; 10.1017/S0022112004009796.

[44] Unified fluid flow model for pressure transient analysis in naturally fractured media; Petro Babak[1] and Jalel Azaiez; Journal of Physics A: Mathematical and Theoretical, Volume 48, Number 17.

[45] Quinn, H. M. Quinn's Law of Fluid Dynamics Pressure-driven Fluid Flow Through Closed Conduits, *Fluid Mechanics*. Vol. 5, No. 2, 2019, pp. 39-71. doi: 10.11648/j.fm.20190502.12.

[46] Jan H. van Lopik1 Roy Snoeijers1 Teun C. G. W. van Dooren1 Amir Raoof1 Ruud J. Schotting; Transp Porous Med (2017) 120: 37–66 DOI 10.1007/s11242-017-0903-3.

[47] Forchheimer, P.: Wasserbewegung durch boden. Zeit. Ver. Deutsch. Ing 45, 1781–1788 (1901).

[48] Quinn, H. M., Quinn's Law of Fluid Dynamics; Pressure-driven Fluid Flow through Closed Conduits. *Fluid Mechanics*. Vol. 5, No. 2, 2019, pp. 39-71. doi: 10.11648/j.fm.20190502.12.

[49] Quinn, H. M., Quinn's Law of Fluid Dynamics: Supplement #2 Reinventing the Ergun Equation. *Fluid Mechanics*. Vol. 6, No. 1, 2020, pp. 15-29. doi: 10.11648/j.fm.20200601.12.

[50] Sidiropoulou, M. G., Moutsopoulos, K. N., Tsihrintzis, V. A.: Determination of Forchheimer equation coefficients *a* and *b*. Hydrol. Process. 21 (4), 534–554 (2007).

[51] Quinn, H. M., Quinn's Law of Fluid Dynamics: Supplement #1 Nikuradze's Inflection Profile Revisited. *Fluid Mechanics*. Vol. 6, No. 1, 2020, pp. 1-14. doi: 10.11648/j.fm.20200601.11.

[52] Banerjee A., Srinivas P., Mritunjay K. S., Selchar C. D., Kumar G. N. P., Modelling of Flow Through Porous Media Over the Complete Flow Regime., Transport in Porous Media. Doi.org/10.1007/s11242-019-01274-2.

[53] G. N. Pradeep Kumar, Dr. P. Srinivas; A Revisit To Forchheimer Equation Applied In Porous Media Flow; International Journal of Research in Engineering and Science (IJRES) ISSN (Online): 2320-9364, ISSN (Print): 2320-9356 www.ijres.org Volume 2 Issue 6 June. 2014 PP.41-53.

[54] Mohammad-Bagher Salahi; Mohammad Sedghi-Asl; and Mansour Parvizi; Nonlinear Flow through a Packed-Column Experiment. Journal of Hydrologic Engineering December 2014. DOI: 10.1061/(ASCE)HE.1943-5584.0001166.

[55] Li, Z., Wan, J., Zhan, H., Cheng, X., Chang, W., Huang, K., Particle Size Distribution on Forchheimer Flow and Transition of Flow Regimes in Porous Media, *Journal of Hydrology* (2019), https://doi.org/10.1016/j.jhydrol.2019.04.026.

[56] J. Mazzeo, U. D. Neue, M. Kele, R. S. Plumb; Analytical Chemistry, December 2005, 460-467.

[57] D. Cabooter, J. Billen, H. Terryn, F. Lynen, P. Sandra, G. Desmet; Journal of Chromatography A, 1178 (2008) 108–117.